

Contents lists available at ScienceDirect

NanoImpact

journal homepage: www.journals.elsevier.com/nanoimpact



Effect of nanomaterial and media physicochemical properties on nanomaterial aggregation kinetics



Mohammed Baalousha

Center for Environmental Nanoscience and Risk, Arnold School of Public Health, University South Carolina, Columbia, SC 29208, United States Department of Environmental Health Sciences, Arnold School of Public Health, University South Carolina, Columbia, SC 29208, United States

ARTICLE INFO

Article history:
Received 24 August 2016
Received in revised form 26 October 2016
Accepted 31 October 2016
Available online 04 November 2016

ABSTRACT

Understanding nanomaterial (NM) stability is required for an adequate interpretation of ecotoxicological test outcomes, fate and behavior studies, to generate parameters (such as critical coagulation concentration, CCC; and attachment efficiency, α) for environmental fate models, and for comparison among different studies. Numerous studies measured CCC and α for different types of NMs with a major focus on investigating the effect of ionic strength, ion valency and natural organic matter, with fewer studies investigating the effect of NM and other medium properties. Consequently, wide discrepancies can be found in the literature among the reported CCC and α values, even for NMs of the same composition and properties. In this context, the aim of this review is to investigate the dependence of NM aggregation kinetic parameters (e.g. CCC and α) on NM and medium physicochemical properties and to rationalize the differences observed among different studies, where possible. We found that various material and medium physicochemical properties need to be considered to predict NM aggregation behavior. Some trends were observed and rationalized based on theoretical studies and data available in the literature. For charge stabilized NMs with constant zeta potential, NM stability (CCC) decreases with the increase in Hamaker constant, increase in NM size, increase in buffer (carbonate and phosphate) concentration, increase in temperature, and light irradiation. The CCC increase with counterion complexation. For sterically stabilized NMs, the CCC increases with the increased surface coverage by the capping agent molecules and completely coated NMs do not aggregate even in high ions strength medium (e.g. seawater). These results highlight the significant role of NM and medium properties in influencing the environmental stability and fate of NMs, and will help refine NM fate models and improve our understanding of NM uptake and toxicity.

© 2016 Elsevier B.V. All rights reserved.

Contents

1.	Introd	Introduction		
2.	Theoretical background			
	2.1.	DLVO theory		
	2.2.	Stability ratio, attachment efficiency, and critical coagulation concentration		
	2.3.	The Schulze-hardy rule		
	2.4.	Stabilization mechanisms and criteria		
		2.4.1. Electrostatic stabilization		
		2.4.2. Steric stabilization		
		2.4.3. Electrosteric stabilization		
	2.5.	Destabilization mechanisms		
3.	. A note on variability of experimental conditions			
4. Effect of medium and environmental physicochemical properties on NM stability				
	4.1.	Counterion, pH and natural organic matter		
	4.2.	Buffer concentration		
	4.3.	Dissolved oxygen		
	11	Limb+		

E-mail address: mbaalous@mailbox.sc.edu.

	4.5.	Temperature			
	4.6.	Chemical interactions of NMs with water constituents			
5.	Effect	of NM physicochemical properties on their stability			
	5.1.	NM composition			
	5.2.	Crystal structure			
	5.3.	Morphology			
	5.4.	Size			
	5.5.	NM dispersity			
	5.6.	Surface area			
	5.7.	Heterogeneity of chemical composition and surface structure			
	5.8.	NM concentration			
	5.9.	Surface coating composition and coverage			
6.	Conclu	uding remarks			
Abb	reviatio	nns			
Acknowledgement					
App	endix A	s. Supplementary data			
Refe	rences.				

1. Introduction

The stability of engineered nanomaterials (NMs) has been studied over the past two decades, since the evolution of nanotechnology. However, the stability of colloidal dispersions has been studied for over a century (Verwey and Overbeek, 1948; Derjaguin and Landau, 1941). A substantial progress in the understanding of the stability phenomena has been made since the introduction of the DLVO theory, which attributed the interaction between two identical particles to van der Waals attraction and the electrical double layer repulsion (Verwey and Overbeek, 1948; Derjaguin and Landau, 1941). Additionally, numerous studies have shown the importance of other interaction forces such as steric forces, and hydration forces on NM aggregation and aggregation kinetics (Baalousha et al., 2011a).

Quantitative assessment of NM stability can be achieved by estimating the attachment efficiency (α) - the inverse of the stability ratio (W) - and the critical coagulation concentration (CCC), which is the minimum counterion concentration required to fully destabilize the dispersion (see details in Section 2) (Tadros, 2007). The aggregation kinetics parameters (α , W, and CCC) of a specific counterion can be calculated theoretically using the classical DLVO theory on the basis of a static force balance. The aggregation kinetic parameters also can be measured experimentally from a kinetic point of view by studying the process of colloidal aggregation (Liu et al., 2009a). This can be achieved by monitoring the growth in NM size, or the loss of UV–vis absorbance for plasmonic NMs (e.g. Au and Ag NMs) at early stage of aggregation (Baalousha et al., 2013).

Numerous aggregation kinetics' experimental studies have focused on investigating the effect of ionic strength, ion valency, pH and natural organic matter (NOM) concentration on NM kinetic stability (CCC and α) (Baalousha et al., 2013; Hotze et al., 2010; Zhou and Keller, 2010; Baalousha et al., 2008; Baalousha, 2009). However, wide discrepancies can be found in the literature among the reported CCC and α values. These discrepancies are likely to be attributed to differences in the experimental conditions among the different studies such as: 1) method employed to investigate NM aggregation kinetics (e.g. DLS, and UV-vis) (Baalousha et al., 2013), 2) physicochemical properties of the NMs (e.g. size, shape, surface coating, etc.) (Penners and Koopal, 1987; Zhou et al., 2013), and 3) media chemistry (e.g. buffer type and concentration, and ligand type and concentration) (Stemig et al., 2014), and 4) environmental factors (e.g. temperature, and irradiation) (Hotze et al., 2010; Zhou and Keller, 2010; Zhou et al., 2013).

There is currently a limited knowledge on the effect of intrinsic properties of NMs (e.g. particle size, morphology, crystal structure, surface heterogeneity, and dopants) and intrinsic properties of the medium (e.g. buffer type and concentration, interaction of NM with medium

constituents, and dissolved oxygen) and environmental factors (e.g. light, and temperature) on NM aggregation (Hotze et al., 2010; Zhou and Keller, 2010; Zhou et al., 2013). For instance, recent studies reported contradictory results on the dependence of CCC on NM size including a decrease with the decrease in NM size (e.g. hematite (He et al., 2008), TiO₂ (Zhou et al., 2013)), an increase with the decrease in NM size (e.g. CdSe (Mulvihill et al., 2010)) or independence of CCC of NM size (e.g. Au and Ag NMs (Liu et al., 2012; Afshinnia et al., 2016a)). In addition, whereas some studies reported a linear correlation between the CCC and NM primary particle size (e.g. anatase TiO2 (Zhou et al., 2013)), other found that the CCC correlated better with NM specific surface area (e.g. anatase TiO₂ (Zhou et al., 2013), CdSe (Mulvihill et al., 2010)). Other studies reported an important role of stabilizing agent (Mulvihill et al., 2010), impurities introduced during synthesis process (Liu et al., 2011), etc. on NM stability. These studies suggest that material properties such as particle size, capping ligand, and impurities are important parameters affecting NMs' aqueous stability. However, a systematic review on the role of NM, and medium intrinsic properties on NM aggregation kinetics is lacking.

Several studies also reported deviations in NM aggregation behavior from classical DLVO behavior. Such deviations have been attributed to a wide selection of causes including discreetness of surface charge (Schudel et al., 1997), steric and relaxation effects (Ortega-Vinuesa et al., 1996), the presence of nanobubbles on particles (Mahnke et al., 1999; Parker et al., 1994; Yakubov et al., 2000), and the inherent surface roughness of the particles themselves (Shulepov and Frens, 1996; Bhattacharjee et al., 1998; Kostoglou and Karabelas, 1995; Sun and Walz, 2001). The deviation of NM aggregation behavior from the classical DLVO theory and the corrections proposed in the literature to the DLVO theory is discussed where relevant in the manuscript.

In this context, this article aims to investigate the relationship between the CCC values and the parameters affecting NM aggregation behavior and kinetics, in particular NM and medium properties. This review focuses on studies reporting NM aggregation kinetics measurement and is organized as follows: 1) a brief review of the key concepts in NM stability (e.g. DLVO theory, Schulze-Hardy rule, α and CCC), 2) a brief discussion of the methods used to measure NM aggregation kinetics (e.g. DLS and UV–vis), 3) a critical discussion on the factors affecting NM aggregation kinetics, together with a rationale for the variability in the reported CCC values for the same type of NM based on NM and media physicochemical properties, and 4) critical discussion on deviations from DLVO theory due to NM specific properties, which is integrated throughout the manuscript.

Understanding of the fate and behavior of NMs in environmental and toxicological media is crucial to allow for comprehensive environmental risk assessment of NMs (Klaine et al., 2008). Aggregation is

one of the key processes, among others, determining their environmental fate, behavior, uptake, effects, etc. (Peijnenburg et al., 2015). Furthermore, understanding the interplay of NM and media physicochemical properties and their aggregation behavior under conditions of ecotoxicological and environmental media is required for an adequate interpretation of ecotoxicological test outcomes, fate and behavior studies, to generate parameters (e.g. α and CCC) (Dale et al., 2015a) for environmental fate models (Dale et al., 2013; Baalousha et al., 2016a; Dale et al., 2015b), and for comparison among different studies.

In this paper, we gathered data from research articles reporting NM aggregation kinetics' experiments and deriving CCC values (Tables S1 and S2). Data on NM properties (size, zeta potential, coating type and concentration, and NM concentration), water properties (pH, buffer concentration, ion type and concentration, concentration and type of NOM) and CCC were extracted and tabulated (Tables S1 and S2). Therefore, this review will act as a repository for CCC values for different types of NMs.

2. Theoretical background

This section briefly summarizes the scientific theories of stability and interactions of NM suspensions to underpin the discussion presented later on in the article. For more details on colloidal science theories and interaction forces between particles, the reader is referred elsewhere (Verwey and Overbeek, 1948; Derjaguin and Landau, 1941; Baalousha et al., 2011a; Bhattacharjee et al., 1998; Baalousha et al., 2011b; Petosa et al., 2010; Elimelech et al., 1995a; Elimelech et al., 1995b).

2.1. DLVO theory

DLVO theory is a fundamental colloidal science theory that was developed by Derjaguin, Landau, Verwey, Overbeek (DLVO) to explain the interaction between colloidal particles. Classical DLVO theory assumes that the total interaction potential (V_T) of two colloidal particles is determined by the sum of the electric double layer repulsions (V_{EL}) and the van der Waals attractions (V_A) (Eqs. (1)–(4)) (Tadros, 2007; Petosa et al., 2010).

$$V_T = V_A + V_{EL} \tag{1}$$

$$V_A = -\frac{rA}{12h} \tag{2}$$

where r is particle radius, A is Hamaker constant of particles in water, h is particle-particle separation

$$V_{EL} = 32\pi\varepsilon r \left(\frac{K_B T}{Ze}\right)^2 \Upsilon^2 \exp(-\kappa h) \tag{3}$$

where ε is the dielectric constant of water, K_B is Boltzmann constant, T is temperature, T is the reduced surface potential, κ is the Debye-Hückel parameter, Z is the valence of ions and e is the elementary charge.

The reduced surface potential, γ , can be calculated using the equation

$$\Upsilon = \tanh\left(\frac{Ze\phi}{4k_BT}\right) \tag{4}$$

where ϕ is the surface potential.

On approach of NMs, the electric double layer results in repulsion that is determined by the magnitude of the surface or zeta potential and electrolyte concentration and valency. The combination of these two forces results in an energy-distance profile (Fig. 1), which can be used to calculate the aggregation rate of two colloidal particles. In agreement with experiment, DLVO theory predicts that charged particle suspensions are kinetically stable at low counterion concentrations and

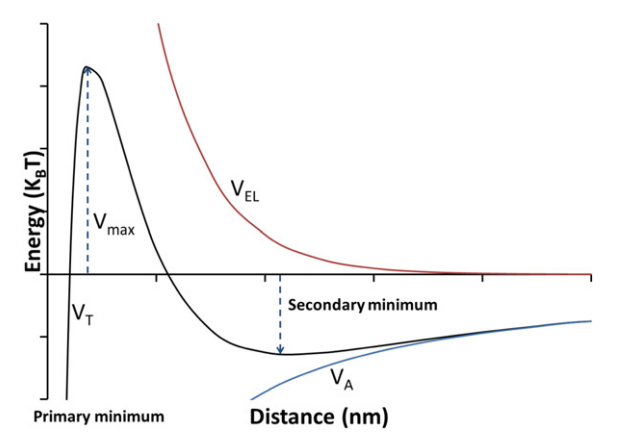


Fig. 1. Energy-distance curve for electrostatically stabilized dispersions.

become unstable at higher counterion concentrations (Chen et al., 2006; Chen et al., 2007). The transition between these two regimes is rather sudden and is referred to as the critical coagulation concentration (CCC), which is the minimum counterion concentration required to fully destabilize the dispersion (Tadros, 2007).

Fig. 1 explains the kinetic stability of colloidal dispersions. For particles to undergo aggregation into the primary minimum, they need to overcome the energy barrier (V_{max}). The higher the value of this energy barrier, the lower is the probability of aggregation, *i.e.* the aggregation rate will be slow. Hence the aggregation process can be considered as a rate (kinetic) phenomenon, also known as reaction limited aggregation (RLA) regime. When the aggregation rate is low enough, the system can remain kinetically stable for months or years, depending on the magnitude of the energy barrier. The aggregation rate increases with the reduction of the energy barrier (due to the reduction in double layer repulsion) and becomes very fast in the absence of the energy barrier. This is also known as diffusion limited aggregation (DLA) regime.

The secondary minimum at long separation distances (Fig. 1) may become deep enough depending on electrolyte concentration, particle size and shape and the Hamaker constant, reaching several k_BT units. Under these conditions, the system becomes weakly flocculated (Tadros, 2007). Aggregation in secondary minimum – when a secondary minimum is of the order of $\it ca.1-5~k_BT$ – is reversible in nature and some disaggregation may occur, $\it e.g.$ under shear force (Tadros, 2007).

The DLVO theory achieved great success in explaining the stability of colloids in electrolyte solutions. Many recent studies have begun applying colloid science principles such as DLVO theory to NMs. However, the novel properties of NMs (e.g. small size, shape, structure, composition, roughness, surface coating and functionalization, etc.) challenged the assumptions of the DLVO theory (Hotze et al., 2010; Cosgrove, 2005; Ninham, 1999; Masliyah and Bhattacharjee, 2006). Assumptions of DLVO theory are summarized below, but the reader is referred elsewhere (Cosgrove, 2005; Ninham, 1999; Masliyah and Bhattacharjee, 2006) for extensive discussion of these assumptions:

- 1- Dispersion is dilute,
- 2- Perfect sphere: the surface is molecularly smooth, solid and spherical,
- 3- The electric charge and other properties are uniformly distributed over the solid surface,
- 4- Only two forces act on the dispersed particles; van der Waals force and electrostatic force. These forces are treated independently and assumed additive,
- 5- Additivity: the net interaction energy between a molecule and planer surface made up of like molecules will be the sum of the interaction energy between the molecule and every molecule in the surface body,
- 6- The ions are point charges, i.e. without any particle size,

- 7- The distribution of ions is determined by the electrostatic force, Brownian motion and entropic dispersion,
- 8- The intervening medium is a structureless continuum, characterized only by its dielectric constant,
- 9- Electrical permittivity is constant through the double layer,
- 10- The solvent is uniform at the atomic level,
- 11- Derjaguin approximation $\kappa r \gg 1$ and $h \gg r$; that is the thickness of the diffuse double layer is much smaller than the particle radius and the separation distance between the particles is much greater than the particle radius.

These assumptions, clearly not all fulfilled in practical colloidal interactions, work quite well for large surface separations $h > \kappa^{-1}$ and large particles, but start to break down at smaller h and r, where an accurate description of the interaction forces should resort to numerical solution of the Poisson Boltzmann equation (Cosgrove, 2005). Further discussion of these limitations is provided in the manuscript where relevant.

2.2. Stability ratio, attachment efficiency, and critical coagulation concentration

Depending on counterion concentration, aggregation occurs in reaction limited or diffusion limited regimes (RLA and DLA, respectively). These two aggregation processes are differentiated by the attachment efficiency (α); ranging from 0 to 1, which defines the probability that two colliding particles attach successfully or irreversibly. In RLA regime, an increase in electrolyte concentration screens the surface charge and reduces the energy barrier (see DLVO theory below) to aggregation, which leads to faster aggregation. At electrolyte concentrations above the CCC, the energy barrier is eliminated resulting in DLA. The CCC is the transition point between the two aggregation regimes. For DLA regime, particles attach to each other after first collision ($\alpha=1$) and form large open fractal aggregates. For RLA regime, particles attach to each other following several collisions (α < 1) and form denser aggregates (Waite et al., 2001).

Theoretically, the DLVO theory can be used to calculate the aggregation kinetic parameters (stability ratio (W), α , and CCC). Under unfavorable conditions (e.g. high zeta potential and low ionic strength), NM aggregation is "slow" or "reaction limited". The W and α for spherical NMs of equal sizes is given by Fuchs equation (Fuchs, 1934)

$$W = \frac{1}{\alpha} = 2r \int_0^{\alpha} \frac{exp\left(\frac{V_{max}}{k_B T}\right)}{\left(2r + h\right)^2} dh$$
 (5)

A simple approximation of this equation is given in Eq. (6) (Elimelech et al., 1995b)

$$\alpha = 2\kappa r \exp\left(-\frac{V_{max}}{k_B T}\right) \tag{6}$$

$$\kappa = \sqrt{\frac{\varepsilon k_B T}{2N_A e^2 I}} \tag{7}$$

where I is the ionic strength of the electrolyte, N_A is Avogadro number, and e is the elementary charge.

Eq. (6) predicts very low attachment efficiencies for energy barrier above few k_BT because of the exponential dependence of α on the energy barrier (V $_{\rm max}$). Eqs. (6) and (7) also predict that small changes in electrolyte concentration can have a dramatic effect on the aggregation rate because κ decrease with the increase in electrolyte concentration.

Experimentally, the stability of any dispersion can be assessed quantitatively by measuring the attachment efficiency (α) - the inverse of the stability ratio (W) - and the critical coagulation concentration (CCC). W (Eq. (8)) is the ratio between the rate of fast aggregation $(k_{\rm f}$, in the absence of energy barrier) to that of slow aggregation $(k_{\rm s}$, in the presence

of energy barrier). CCC is the minimum counterion concentration required to fully destabilize the dispersion; that is to induce rapid NM aggregation (Tadros, 2007). In general, W, α , and CCC are experimentally determined from the dependence of the aggregation rate on counterion concentration (C_E).

$$\alpha = \frac{1}{W} = \frac{k_s}{k_f} \tag{8}$$

There are a few approaches for determining CCC experimentally including: (1) approaches based on measuring the aggregation rate constant and the attachment efficiency (α) including direct counting of aggregates with ultramicroscope or particle counter (Matthews and Rhodes, 1968; Gedan et al., 1984; Cahill et al., 1986; Pelssers et al., 1990; Broide and Cohen, 1992), turbidity measurements (Ottewill and Shaw, 1966; Reerink and Overbeek, 1954; Lichtenbelt et al., 1974a; Lichtenbelt et al., 1974b; Trompette and Meireles, 2003), NM aggregate diffusion coefficient (size) measurement by static light scattering (Lips et al., 1971; Lips and Willis, 1973; Giles and Lips, 1978; Zeichner and Schowalter, 1979), dynamic light scattering (DLS) (Virden and Berg, 1992; Novich and Ring, 1985; Einarson and Berg, 1993; Nur et al., 2015), fluorescence correlation spectroscopy (FCS), and absorbance of primary particles by UV-vis (Baalousha et al., 2013). DLS is by far the most commonly used method for monitoring NM aggregation. However, these methods still have their own limitations (Gregory, 2009). (2) Approaches based on measuring the sedimentation rate which can be obtained from the determination of the percent transmittance of the supernatant after 24 h sedimentation (Burns et al., 1997; Saejiew et al., 2004; Frenkel et al., 1992; Hesterberg and Page, 1990). The gravitational sedimentation methods have now been recognized to be complicated, cumbersome, and unreliable, and therefore have been recently replaced by the DLS measurements. Full discussion of these approaches is beyond the scope of this article, however extensive discussion of these approaches can be found elsewhere (Gregory, 2009).

2.3. The Schulze-hardy rule

The Schulze-Hardy rule is an empirical rule stating that: the CCC of hydrophobic sols is extremely sensitive of the valence of the counterion, and decreases very strongly with the increased valence of the counterion (Matijevic and Allen, 1969; Vincent, 2012). The Schulze-Hardy rule suggests that the destabilizing power of an electrolyte is principally due to the valence of its ion that has charge opposite to NM surface (counterion), whereas the nature and valence of its ionic species with the same sign (co-ions) have relatively little effect. For this reason trivalent salts of aluminum and iron are the most widely used inorganic coagulants in water clarification and wastewater treatment (Nowicki and Nowicka, 1994).

The theoretical explanation of this rule had to wait the development of the DLVO theory. Verwey and Overbeek introduced the following criteria for transition between stability and instability (Tadros, 2015):

$$V_T = V_{El} + V_A = 0$$

$$\frac{dV_T}{dh} = 0$$

Solving Eq. (5) for these boundary conditions results in

$$CCC \propto \frac{1}{A^2 Z^6} tanh^4 \left(\frac{Ze\zeta}{4K_B T} \right) \tag{9}$$

Eq. (9) shows that the CCC increase with the increase in zeta potential (ζ), and decrease with increasing A (the Hamaker constant) or van der Waals attraction and it also decreases with increase in counterion valency, Z. This equation shows that for large ζ and symmetric Z:Z

electrolyte (*i.e.* $\frac{Ze\zeta}{4K_BT}\gg 1$, $tanh^4(\frac{Ze\zeta}{4K_BT})\to 1$), the CCC is proportional to Z^{-6} . However, for low ζ and symmetric Z:Z electrolyte (*i.e.* $\frac{Ze\zeta}{4K_BT}\ll 1$, $tanh^4(\frac{Ze\zeta}{4K_BT})\to (\frac{Ze\zeta}{4K_BT})^4$), which are common for NMs, the CCC is proportional to Z^{-2} . In practice, the CCC dependence on Z for a wide range of NMs should be between Z^{-6} and Z^{-2} (Petosa et al., 2010). Therefore, for the majority of NMs, the $CCC_{divalent}/CCC_{monovalent}$ ratio lies between 4 and 64

Several studies verified the applicability of Schulze-Hardy rule. For instance, Au NMs have been shown to follow the Schulze-Hardy rule for monovalent, divalent and trivalent electrolytes (Nowicki and Nowicka, 1994). Hematite NMs were shown to follow the Schulze-Hardy rule for monovalent, divalent and trivalent electrolytes; whereas humate-coated hematite NMs followed the Schulze-Hardy rule for monovalent and divalent electrolytes only and deviated for trivalent electrolytes. This behavior was attributed to the relatively strong complexation of humate (Verrall et al., 1999).

2.4. Stabilization mechanisms and criteria

NMs are typically stabilized by either an electrostatic (*i.e.* charge-based) repulsion or a steric repulsion by surface coating (*i.e.* engineered or incidental), or a combination of both (*i.e.* electrosteric), in which case surface coating can further stabilize NM by steric stabilization in addition to charge repulsion (Fritz et al., 2002; Roucoux et al., 2002).

2.4.1. Electrostatic stabilization

Electrostatically-stabilized NMs owe their stability to particle charge, which results in the formation of diffuse double layer around NMs. Any constituent which influences the surface charge will also change NM stability. The most profound effect is exercised by ions of charge opposite to that of NMs, which result in charge screening and shrinkage of the diffuse double layer thickness. The condition of colloid stability of charge stabilized NMs is to have an energy barrier that is much greater than the thermal energy of the particles (which is of the order of $k_B T$). As a rule of thumb, the energy barrier should be typically ${>}25\ k_B T$. This can be achieved by having a high zeta potential (ca. typically ${\mid}\zeta{\mid}{>}40\ mV$) and low electrolyte concentration (ca. typically ${<}100\ mM$ 1:1 electrolyte).

2.4.2. Steric stabilization

Steric stabilization refers to the stabilization of colloidal particles against aggregation by nonionic macromolecules e.g. polymers (Napper, 1977). When two particles having an adsorbed polymer layer with a hydrodynamic thickness δ_H approach each other to a surface-surface separation distance h that is smaller than $2\delta_h$, the polymer layers from the two particles interact resulting in two main situations; either the polymer chains may overlap or the polymer layer may undergo some compression. In both cases, there will be an increase in the local segment density of the polymer chains in the interaction zone. This local increase in segment density in the interaction zone will result in strong repulsion as a result of two main effects (Hiemenz and Rajagopalan, 1997):

- 1- Restriction of adsorbed polymer chain motion, which causes a decrease in entropy and thus an increase in free energy. This entropy reduction results from the decrease in the volume available for the polymer chains whether these chains are overlapped or compressed.
- 2- Increase in the osmotic pressure as the solvent will reestablish the equilibrium by diluting the polymer chains and thus separating the particles.

The criteria for effective steric stabilization are (Tadros, 2007):

• The particles should be fully covered by the polymer. Any bare patches may cause aggregation either by van der Waals attraction between the bare patches or by bridging. The latter occurs when polymer

- becomes simultaneously adsorbed on two or more particles.
- The polymer should be strongly adsorbed to the particle surface. Desorption or replacement of the surface coating by molecules/ligands with high affinity to particle surface could compromise NM stability (Afshinnia et al., 2016b).
- The stabilizing chain should be highly soluble in the medium and strongly solvated by its molecules.
- The adsorbed layer thickness should be sufficiently large to maintain shallow minimum. This is particularly the case when a colloidally stable dispersion without any weak aggregation is required (Tadros, 2007).

2.4.3. Electrosteric stabilization

Electrostatic and steric stabilization can be combined to maintain the NM stability, which is also referred to as electrosteric stabilization. This kind of stabilization is generally provided by means of ionic surfactants. These compounds bear a polar head group able to generate an electric double layer and a lypophilic side chain able to provide steric stabilization. The adsorption of charged, high molecular weight molecules such as NOM also provides electrosteric stabilization (Baalousha et al., 2013; Baalousha et al., 2008; Baalousha, 2009).

2.5. Destabilization mechanisms

The destabilization of colloidal suspension can be accomplished by two different mechanisms: 1) processes that induce a reduction in the total potential energy of interaction between the electrical double layers of two similar particles and 2) processes that aggregate colloidal particles by the formation of chemical bridges (Stumm and O'Melia, 1968). The first mechanism can be achieved by surface charge screening by a counterion, or by surface coating replacement (e.g. a charged coating by a neutral coating) (Moskovits and Vlc ková, 2005). The second mechanism can be achieved by chemical sorption of organic compounds, formation of inorganic complexes, and precipitation of inorganic salts. These interactions can significantly impact NM surface charge and aggregation kinetics and results in significant changes in CCC and α .

So far, a significant attention has been giving to investigating the impact of water physicochemical parameters such as ionic strength, cation type, and valency, pH, and NOM concentration and type on NM aggregation kinetics (Tables S1 and S2) (Baalousha et al., 2008; Baalousha, 2009). However, little attention has been giving to chemical interactions that may affect NM aggregation kinetics. Natural waters, cell growth media as well as toxicological media are rich in other constituents than those listed above such as anions (e.g. PO_4^{3-} , CO_3^{2-} , Cl^{-}), and biomolecules (e.g. cysteine, cystine, glutathione, proteins, enzymes, vitamins, glucose, etc.) (Metreveli et al., 2016a), and pH buffers (e.g. carbonate, phosphates, Tris, HEPES, etc.). Chemical interaction between NM surfaces and medium constituents leads to the formation of ligandmetal complexes, core-shell NMs and chemical sorption of macromolecules, which will alter NM surface charge and thus overall stability. For instance, taking silver as example, this includes, but not limited to, formation of AgCl, Ag₂CO₃, Ag₃PO₄, and Ag-cysteine complexes.

3. A note on variability of experimental conditions

Crucial to improving the understanding of the factors controlling NM aggregation kinetics is to establish meaningful comparison between results obtained by different research groups. A survey of recent research articles in the field reveals substantial variation in experimental conditions (Tables S1 and S2). Variations include NM size, dispersity, morphology, surface area, surface roughness, composition, crystal structure, concentration, surface coating type and concentration, buffer concentration, electrolyte type and concentration, dissolved oxygen (DO), light, and temperature, and consequently CCC values. Ag NMs

are the most widely studied NMs in the literature with the largest number of articles reporting CCC values under variable NM and media properties (Table S1), and full statistical analysis of these data is provided elsewhere (Afshinnia et al., 2017). pH was generally around neural conditions (ca. 6.0–8.0), except few studies (Chen et al., 2006; Liu et al., 2010). Citrate was the most investigated capping agent among others such as SDS, alginate, PVP, casein, dextrin, tween, branched polyethyleneimine (BPEI), and Gum Arabic (Table S1 and S2). Parameters such as NM size, buffer concentration have rarely been investigated (Afshinnia et al., 2016a; Afshinnia and Baalousha, 2016). Below we rationalize the differences in the CCC values based on the variability in the experimental conditions, which includes NM and medium physicochemical properties.

4. Effect of medium and environmental physicochemical properties on NM stability

4.1. Counterion, pH and natural organic matter

The large majority of NM aggregation kinetics investigated the effects of counterion valence, pH and NOM on NM aggregation kinetics (see Tables S1 and S2). There is currently a consensus that divalent counterions are more effective in screening NM surface charge than monovalent counterions, in agreement with Schulze-Hardy rule (Nowicki and Nowicka, 1994; Verrall et al., 1999; Hall et al., 1991). For electrostatically stabilized NM, the CCC of an electrolyte depends strictly on the counterion valence, as long as the adsorption of the co-ion or the counterions on the surface is negligible. Under this condition, the Schulze-Hardy rule is obeyed. If an ion adsorbs sufficiently strongly on the surface of NMs at concentrations lower than the CCC, the Schulze-Hardy rule does not apply (Matijevic and Allen, 1969). This is because specific scorpion of ions on the surface of NM will alter their surface potential. The majority of studies on electrostatically stabilized NMs reported CCC values for monovalent and divalent electrolytes (Table S1 and S2) within the boundaries of the Schulze-Hardy rule; that is the ratio of the CCC of monovalent to that of divalent counterions varies within the range 4 to 64.

NOM (typically Suwannee River fulvic and humic acids) sorb on the surface of NMs, increase their zeta potential, impart NM electrosteric stabilization, and increases the CCC by *ca.* 1–5 folds (Tables S1 and S2). Additionally, several studies have demonstrated that NOM results in a reduction in the Hamaker constant (Baalousha et al., 2013; Huynh and Chen, 2011; Amal et al., 1992).

pH plays an important role in controlling NM aggregation kinetics by determining NM zeta potential. For instance, the CCC of ZnO (Zhou and Keller, 2010) and TiO₂ (Snoswell et al., 2005) NMs increases as the pH was further away from the point of zero charge (pH_{PZC}). Nonlinear monotonic relationships were found between the CCC and either pH-pH_{PZC} or electrophoretic mobility (EPM) (Zhou and Keller, 2010). This is because, further away from the pH_{PZC}, ZnO NMs possess a larger zeta potential; therefore, higher ionic strength is needed to screen the surface charge and reduce the electrostatic repulsion between NMs.

4.2. Buffer concentration

Buffers are usually used to maintain a constant pH during a reaction, but their presence can result in substantial changes in NM surface chemistry (e.g. formation of a core-shell particles, or alteration of zeta potential) (Buchholz et al., 2011) and therefore NM stability (Stemig et al., 2014; Liang, 1988). For instance, goethite NMs aggregate size increased with increased MOPS (3-Morpholinopropanesulfonic acid) buffer concentration. This behavior was attributed to sorption of MOPS molecules on the surface of goethite NMs accompanied by a decrease in zeta potential (Stemig et al., 2014). Furthermore, the buffer composition greatly affects goethite NMs aggregation state. Goethite NMs suspended in solution containing 1 mM Fe²⁺ and HEPES buffer

were the most dispersed, and the aggregate sizes were 3-5 times larger for goethite NMs suspended in MOPS and Triethanolamine (TEA) buffers compared to those suspended in HEPES buffer (Stemig et al., 2014). The stability of hematite particles decrease in the presence of phosphate anions (Liang, 1988). Furthermore, the CCC values for electrostatically stabilized Ag NMs decrease with the increase in carbonate buffer concentration (Afshinnia et al., 2017) and phosphate buffer (Afshinnia and Baalousha, 2016). This behavior was attributed to the formation of Ag₂CO₃, or Ag₃PO₄ layer on the surface of Ag NMs, altering NM surface charge (Afshinnia and Baalousha, 2016). For a constant Ag NM concentration (5.4 mg L^{-1}), zeta potential increased from -42 mV to -29 mV with the increase in phosphate buffer concentration from (0 to 2.5 mM potassium phosphate monobasic) (Afshinnia and Baalousha, 2016). Another study demonstrated that, at pH 7, the zeta potential of Ag NMs increases (become less negative) with the decrease in NM concentration (1 to 100 µM) in 10 mM carbonate concentration (Piccapietra et al., 2012). Concurrently, Ag NM aggregate size increases with the decrease in NM concentration. This behavior can be attributed to the increased sorption of CO₃⁻² on the surface of Ag NMs at lower NM concentrations due to the increased abundance of CO_3^{-2} anions compared to the NM total surface area.

4.3. Dissolved oxygen

Dissolved oxygen (DO) in aqueous environments tends to oxidize metallic NMs such as Ag NMs and QDs (Zhang et al., 2011a; Li et al., 2012; Zhang et al., 2011b; Liu and Hurt, 2010) resulting in the formation of surface oxide layer (e.g. AgO (Römer et al., 2016)), release of metallic cations (Li et al., 2012; Römer et al., 2016; Ho et al., 2010), and NM aggregation (Zhang et al., 2011a; Li et al., 2012; Li et al., 2013). For instance, the aggregation rate of Ag NMs is much faster (e.g., 3-8 times depending on the primary particle size) in the presence of DO than those in the absence of DO (Zhang et al., 2011a). The increased aggregation of Ag NMs in the presence of DO was attributed to surface oxidation and sorption of Ag⁺ on Ag NM surface (Zhang et al., 2011a). These processes could lead to increase (become less negative) Ag NM zeta potential, hence the increased aggregation rate (Misra et al., 2013). Furthermore, NM aggregation can be attributed to the degradation/detachment of surface coating in the presence of oxygen. For instance, the destabilization of Ag NMs, CdS NMs and QDs was found to be related to the detachment/degradation of surface coating in the presence of oxygen, compression of EDL and surface energy changes (Li et al., 2012; Li et al., 2013; Correa-Duarte et al., 1998). In contrast, anoxic and anaerobic conditions exert low redox potentials, which inhibit oxidation and consequently lead to different aggregation kinetics (Li et al., 2012; Li et al., 2013).

4.4. Light

Light irradiation including UV, sunlight and even fluorescent light has been shown to promote NM surface oxidation, dissolution and aggregation (Mittelman et al., 2015; Gorham et al., 2012; Shi et al., 2013). The CCC of NaNO3 was found to be lower for citrate-Ag NMs following 3-day exposure to UVA and UVB radiation (ccc = 37.8 and 21.4 mM NaNO3) compared with unexposed cit-Ag NMs (ccc = 161.4 mM NaNO3). This decrease in the CCC was concurrent with the increase in the ζ potential (become less negative) after exposure to UVA and UVB (Mittelman et al., 2015). The aggregation rate of bared-, citrate-, and PVP-Ag NMs followed the order UV-365 > xenon lamp light > UV-254 > dark for the same type of Ag NMs, which indicated that the wavelength and photo-energy of the light irradiation influence Ag NM aggregation kinetics (Li et al., 2013). The aggregation rate was highest for bare-Ag NMs followed by citrate Ag NMs and PVP Ag NMs.

UV irradiation of a TiO_2 NM suspension accelerated NM aggregation, which was dependent on the irradiation duration. The aggregation rate increased from <0.001 nm s $^{-1}$ before irradiation to 0.027 nm s $^{-1}$ after

50 h irradiation, resulting in aggregates with a hydrodynamic diameter of 623 nm. The isoelectric point of the suspension was lowered from 7.0 to 6.4 after irradiation. ATR-FTIR spectra displayed successive growth of surface hydroxyl groups (oH $^-$) with UV irradiation which is likely to be responsible for the decreased surface charge and increased aggregation rate. Further explanations of the light-induced ζ potential reduction is described in Sun et al. (2014).

On the other hand, irradiation could result in breakage of NM aggregates (disaggregation). For instance, sunlight partially disaggregated metal oxide (e.g. CeO₂ and ZnO) aggregates, but primary particles bonded by solid state necks remained intact (Zhou et al., 2012). Localized heating of NM agglomerates, due to exposure to natural or artificial light, provides sufficient thermodynamic energy for the clusters to disagglomerate (Zhou et al., 2012). Similarly, Bennett and coworkers found that different light sources (e.g. sunlight or Xenon lamp light) exposure can partially disaggregate TiO₂ NMs aggregates; TiO2 NM aggregate size decreased from about 280 nm to about 230 nm after few minutes' exposure to light, and returned to 280 nm in the dark (Bennett et al., 2012). The photo-induced disaggregation was more pronounced (aggregate size decreased from 253 nm to 159 nm after 30 min exposure) under natural sunlight conditions. The absorption of light provides enough energy to partially disaggregate TiO2 NMs in aqueous media, releasing small particles from the larger aggregates. Concurrently, the dermal transport of NMs was higher (200 mg kg⁻¹) under light conditions compared to dark conditions (75 mg kg⁻¹), suggesting that photo-induced disaggregation may have important health implications (Bennett et al., 2012).

4.5. Temperature

Understanding the temperature effect on NM aggregation kinetics is important to understand NM behavior in environmental and biological media and to understand NM behavior within the context of climate change. Both natural water and human body fluids can be at temperatures that are remarkably different from the typically studied room temperature. For example, water temperature may vary substantially from freezing point to near boiling depending on the type of water body, depth, season, latitude and the surrounding environment. Temperature of human body fluids is around 37 °C.

The aggregation rate of CeO_2 NMs in KCl and $CaCl_2$ increased as the temperature increased. The CCC decreased from 100 to 10 mM in KCl and from 10 to 2 mM in $CaCl_2$ with temperature increase from 4 to 37 °C (Fig. 2) (Chen et al., 2012). The decrease in CCC in KCl shows a linear correlation with the increase in temperature; whereas in $CaCl_2$, the CCC remained constant at 10 mM until the temperature reached 25 °C and then decreased to 3 mM at 37 °C. Similarly, the increase in temperature from 25 to 70 °C resulted in a decrease (67%, 50%, and 33% for Na⁺, $CaCl_2$), and Cal_2 , respectively) of the CCC for silica NMs (25 nm), which was attributed to the increased collision frequency of the colloidal

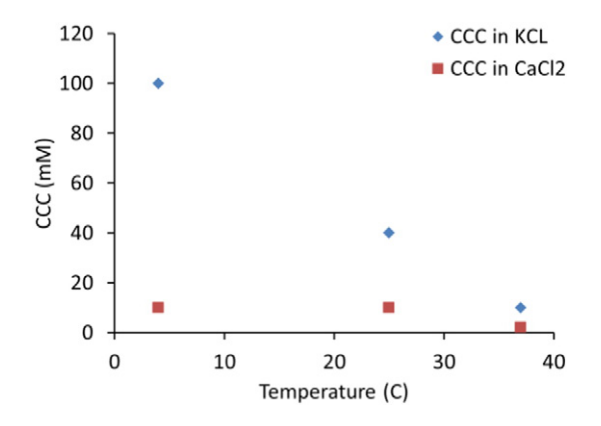


Fig. 2. Effect of temperature on the CCC of CeO₂ NMs. Taken from Chen et al. (2012).

particles at higher temperatures, which promotes successful particle collision and aggregation (Metin et al., 2010). However, increased NM collision frequency does not explain the reduction in CCC. Additionally, according to Eq. (9), for low ζ which are common for NMs and symmetric Z:Z electrolyte (i.e. $\frac{Ze\zeta}{4K_BT}\ll 1$, $\tanh^4(\frac{Ze\zeta}{4K_BT})\to (\frac{Ze\zeta}{4K_BT})^4$). This implies that if all other parameters are constant, the CCC is proportional to T^{-4} . The dependence of CCC on medium temperature does not fully explain the reduction in CCC with the increase in temperature as observed above. The reduction in CCC is likely to be also influenced by the reduction in zeta potential of silica NMs, which unfortunately was not reported by the authors for the different temperatures. Other studies reported decreased stability and increased in NM aggregate size (e.g. CuO (Misra et al., 2011), ZnO (Majedi et al., 2014), and single wall carbon nanotubes (Adeleye and Keller, 2014)) with the increase in temperature.

The increased NM aggregation with the increase in water temperature is likely to be due to the decrease in the magnitude of the zeta potential with the increase in temperature, which was reported for different types of NMs such as ZnO (Majedi et al., 2014), CuO (Misra et al., 2011), TiO₂ (Zhou et al., 2012), single wall carbon nanotubes (Adeleye and Keller, 2014), α -Al₂O₃ (Valdivieso et al., 2006), mineral particles (e.g. quartz, kaolinite and calcite) (Rodríguez and Araujo, 2006). The surface charge of NPs in aqueous medium is mainly determined by two phenomena, protonation/de-protonation of surface functional groups, and adsorption of electrolyte ions on the surface (Borghi et al., 2013). The temperature-dependent decrease in zeta potential is attributed to the changes in NM surface speciation (e.g. protonation or deprotonation of functional groups) with temperature. For instance, increasing temperature favors proton desorption from the α-Al₂O₃ surface, resulting in a shift in the pH_{pzc} of α -Al₂O₃ from 9.6 to 8.1 as the temperature increases from 10 to 40 °C (Valdivieso et al., 2006).

On the other hand, high temperatures may increase the potential disaggregation or detachment of NMs, because increased Brownian motion of water molecules could increase the hydrodynamic shear on the particle surface and possibly break the weakly attached aggregates (Zhou et al., 2012; Ryan and Elimelech, 1996; Zhang et al., 2012a). This behavior was previously reported for metal oxide NMs such as CuO (Misra et al., 2011), CeO₂ (Zhou et al., 2012; Zhang et al., 2012a; Li et al., 2011), iron (III) oxyhydroxide (Gilbert et al., 2009), TiO₂ and ZnO NMs (Zhou et al., 2012). For instance, a cyclic temperature increase from 25 °C to 65 °C and then decrease back was found to disaggregate the NM aggregates in the heating phase and re-aggregate them as more open fractal structures during the cooling phase (Zhou et al., 2012).

4.6. Chemical interactions of NMs with water constituents

Despite its importance in determining NM surface charge, chemical sorption of macromolecules and ligands (e.g. PO_4^{3-} , CO_3^{2-} , Cl^{-}) has been somewhat widely ignored in studying NM aggregation kinetics as the large majority of these studies focused on the physical interactions between NMs. However, emerging studies have reported the importance of chemical interactions in addition to physical interactions in controlling NM aggregation kinetics (Metreveli et al., 2016b; Pokhrel et al., 2013; Wang et al., 2013; Zakaria et al., 2013; Doyen et al., 2016; Chegel et al., 2012; Gebauer et al., 2012; Lesniak et al., 2013). For instance, the CCC for citrate-Ag NMs decreases with the increased concentration of carbonate and phosphate anions in the medium, which was ascribed to the sorption of phosphate and carbonate anions on the surface of citrate-Ag NMs, and the concurrent reduction in the magnitude of Ag NM zeta potential (Afshinnia et al., 2017; Afshinnia and Baalousha, 2016). Addition of cystine to citrate-Ag NMs results in NM concentration-dependent shift in the CCC, where the CCC of cystine decreases with the decrease in Ag NM concentration (Afshinnia et al., 2016b). At lower Ag NM concentrations, lower concentration of cystine is required to fully cover and destabilize Ag NMs

(Afshinnia et al., 2016b). Organic compounds containing both thiol and amine groups strongly promote the aggregation of citrate-Au NMs due to their cooperative functionalities (Chegel et al., 2012). Three features of organic compounds could influence citrate-Au NMs (and similarly Ag NMs) aggregation kinetics including: the presence of a sulfur atom, which can form covalent bonds with gold atoms, the presence of ionizable functional groups, and the sign (+ or -) of ionizable functional groups, which determines the Au NM zeta potential (Chegel et al., 2012). Specific sorption of Ca^{2+} and Mg^{2+} on the surface of TiO_2 NMs results in surface charge inversion (Loosli et al., 2015), which was found to increase the destabilization of TiO_2 NMs (Shih et al., 2012).

Furthermore, complexation of the counterion in complex aqueous media may result in an increase in the measured CCC values. For instance, the CCC of aluminum for negatively charged silver iodide sols was found to increase if the sol was acidified by sulfiric acid; whereas this behavior was not observed when the sol was acidified by nitric acid or perchloric acids (Matijevic and Stryker, 1966). This behavior was attributed to the formation of AlSO₄⁺ complexes in the presence of sulfiric acid, resulting in the reduction in the concentration of trivalent counterion (AlSO₄⁺) and the formation of monovalent counter ion (AlSO₄⁺) (Stryker and Matijevic, 1969). Monovalent counterions are orders of magnitude less potent than trivalent counterions in inducing particle aggregation according to Schulze-Hardy rule. This study reveals the importance of considering counterion speciation in interpreting the discrepancies in CCC.

Clearly, focusing only on the physical interactions (e.g. attraction and repulsion) of NM when taking into account water chemistry in modeling NM environmental fate and behavior (Sani-Kast et al., 2015) might lead to erroneous conclusions as many other parameters can play a major role in determining NM aggregation kinetics - such as anions, buffers, small organic compounds, salt precipitation, etc. - and thus fate and behavior. Therefore, the chemical speciation of counterions and the chemical interaction between NMs and the medium constituent should be fully taken into account to improve our understanding of NM fate and behavior.

5. Effect of NM physicochemical properties on their stability

5.1. NM composition

Chemical composition affects NM aggregation as it determines the Hamaker constant; (Hotze et al., 2010) a material specific constants, typically on the order of 10^{-21} – 10^{-19} J (Table 1) (Pinchuk and Jiang, 2015), that is used to calculate the van der Waals attraction forces between small particles (see Section 1.2). The increase in the Hamaker constant results in an increase in the van der Waals attraction force and therefore the tendency of NM to form aggregates at the same solution and surface chemistry. Therefore, the increase in the Hamaker constant results in a decrease in the CCC and in a steeper slope of the α -

Table 1Hamaker constant of different materials.

Material	A (×10 ⁻²⁰ J)	References
Gold	9–30	(Wijenayaka et al., 2015; Kim et al., 2008; Kim et al., 2005)
TiO ₂	9.1	(Zhang et al., 2009; Zhang et al., 2008)
CeO_2	5.57	(Karimian and Babaluo, 2007)
Cit-Ag NMs	3.7	(Baalousha et al., 2013; Huynh and Chen, 2011)
Al_2O_3	3.67	(Karimian and Babaluo, 2007)
Iron oxides	3.3-3.9	(Zhang et al., 2009; Zhang et al., 2008; Faure et al., 2011)
ZnO	1.9	(Zhang et al., 2009; Zhang et al., 2008)
Boron	0.88	(Liu et al., 2009b)
SiO ₂	0.83-1.2	(Trompette and Meireles, 2003; Zhang et al., 2009; Zhang et al., 2008)

electrolyte concentration profile under RLA regime (Fig. 3a and b). According to Eq. (9), for a constant zeta potential, the CCC is inversely proportional to the squared Hamaker constant, *CCC* α $\frac{1}{A^2}$. Therefore, the CCC of different types of NMs of the same physicochemical properties and in the same medium will follow the order Au < TiO₂ < Ag < Fe₂O₃ < ZnO < SiO₂ (Fig. 3a). Due to the variability in the experimental conditions and the dependence of the CCC on other material and media properties (Afshinnia et al., 2017), it is not possible to verify this order of CCC for all types of NMs. However, this trend can be observed clearly for some NMs; in particular, the CCC of monovalent electrolyte at nearly similar zeta potential values for SiO₂ (450–700 mM) > B (200 mM) > Ag (25–200 mM) (Tables S1–S2).

The Hamaker constant is long thought to be size-independent. However, recent theoretical calculations demonstrate that the Hamaker constant of 1 nm Ag- and Au NMs increases by approximately 15% compared with 100 nm Ag and Au NMs (Pinchuk and Jiang, 2015; Pinchuk, 2012). Another theoretical study demonstrated that the Hamaker constant of a 13 nm diameter Au NMs increases by up to 50% compared with that of bulk gold, causing such small NMs to exhibit larger van der Waals attractive interactions and aggregate more readily than larger particles (Wijenayaka et al., 2015). The increased aggregation of smaller NM would occur if no other properties (*e.g.* surface charge, crystallographic phase, surface facets, dissolution, *etc.*) are affected by particle size (Wijenayaka et al., 2015).

5.2. Crystal structure

Crystal structure such as crystal phase, surface facets and defects can alter surface charge, and thus NM aggregation kinetics (Kosmulski, 2002). The surface charge of different polymorph of the same NM may be different. For example, TiO₂, with three phases of crystallinity, has surface charge of -35 mV for rutile and -20 mV for anatase and brookite at pH 7.5. The origin of charge heterogeneities is commonly attributed to the existence of different crystallographic planes within each particle, which is reported to affect aggregation and deposition rates (Buettner et al., 2010; Gaboriaud and Ehrhardt, 2003). This is because different crystallographic planes, each with a different atomic density, are interfacing with the aqueous phase and forming different extent of EDL and surface energy. For instance, the point of zero charge of goethite particles having 70% and 30% of the 001 face were 9.0 and 9.1 respectively, which was attributed to the differences in the point of zero charge of the 001 and 101 facets, which was calculated theoretically to be 8.9 and 9.2, respectively (Gaboriaud and Ehrhardt, 2003). Crystal structure also affects the Hamaker constant, and thus the attractive van der Waals forces (French et al., 1995). For instance, the magnitude of van der Waals interactions varies significantly between iron oxide phases and follow the order magnetite < maghemite < hematite (Faure et al., 2011). This is because the Hamaker constant depend on the phase and follows the order magnetite (3.3 $\times\,10^{-20}\,\text{J})\,{<}\,\text{maghemite}$ $(3.6 \times 10^{-20} \text{ J}) < \text{hematite } (3.9 \times 10^{-20} \text{ J}) \text{ (Faure et al., 2011)}.$

5.3. Morphology

There are only few studies that investigated the effect of NM morphology on their aggregation kinetics with inconclusive general conclusions. Whereas some studies demonstrated strong effect on NM morphology on their aggregation kinetics (e.g. ZnO (Zhou and Keller, 2010)), others reported no effect (e.g. TiO₂ (Liu et al., 2011)). For instance, the aggregation kinetics of nearly spherical ZnO exhibited strong dependence on the ionic strength of the solution; whereas minimal influence of ionic strength was observed on the irregularly shaped (mixtures of slab-like and rod-shaped) ZnO NMs (Zhou and Keller, 2010). The CCC for nearly spherical ZnO was approximately 25 mM; whereas the CCC for irregularly shaped ZnO was below 1 mM. This behavior was attributed to lower energy barrier for irregularly shaped NMs

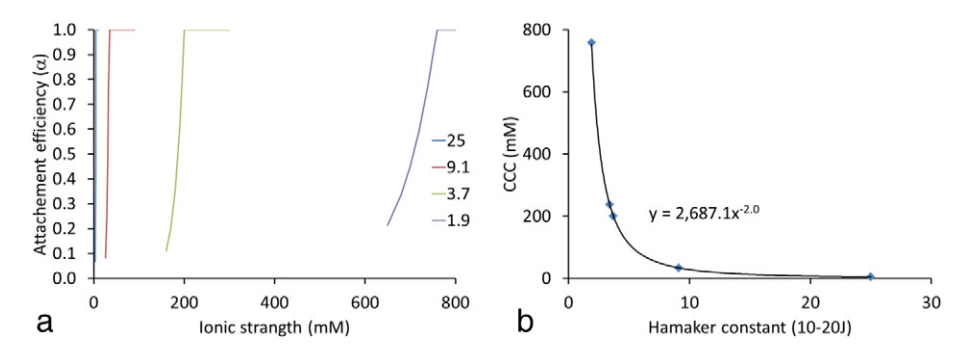


Fig. 3. Effect of material composition (Hamaker constant) on their aggregation kinetics according to classical DLVO theory: (a) attachment efficiency as a function of ionic strength, and (b) CCC as a function of Hamaker constant. Calculations were performed assuming a particle diameter of 20 nm and a constant zeta potential of -50 mV. These calculations are only illustrative.

compared to spherical NMs. Vold (1954) estimated that plates and rods would have greater van der Waals attractions compared with spheres at small separation distances (Vold, 1954), resulting in a lower energy barrier against aggregation.

However, another study suggested that the CCC for TiO $_2$ NMs (5, and 50 nm spherical anatase and 10×40 nm rutile rods) is independent of particle morphology and crystal structure (Liu et al., 2011) as the CCC (10 mM NaCl and 0.5 mM CaCl $_2$) value for 10×40 nm rutile rods was between those of the 5 nm (5 mM NaCl and 0.3 mM CaCl $_2$) and 50 nm (18 mM NaCl and 1.0 mM CaCl $_2$) spherical anatase. The differences in the conclusions drawn by Lie et al. (Liu et al., 2011) and Vold et al. (Vold, 1954) were attributed to the difference in the aspect ratios of the studied rods.

Morphology is likely to play an important role in controlling NM aggregation kinetics, as morphology determines NM zeta potential and isoelectric point (pH_{iep}). This is because different surface facets possess different zeta potentials and pH_{iep}. For instance, the pH_{iep} of TiO₂ surface facets follows the order (100) surface 3.2-3.7 < (110) surface 4.8-5.6 < (001) surface 5.6 - 5.8. Polycrystaline surfaces of both rutile and anatase forms of TiO₂ possess the same pH_{iep} of \approx 6, resulting from the weighted average of the PZC of the single crystal facets (Bullard and Cima, 2006). Similarly, the double-layer properties of (110)-oriented CaF₂ (Assemi et al., 2006) indicated a sharp contrast between the pH_{iep} of that surface and the previously measured (111) orientation (Fa et al., 2003; Oberndorfer and Dobiáš, 1989). Other works has noted anisotropy among hematite surfaces (Hiemstra and van Riemsdijk, 1999) and distinctions between numerous surface chemistries (Fa et al., 2005), and differences in various orientations of sapphire surfaces have also been investigated (Kershner et al., 2004). Therefore, the variability in the reported NM pH_{iep} can be partially attributed to the relative contribution of surface facets to each type of NM.

5.4. Size

There is a contradictory evidence on the dependence of CCC on NM size including a decrease with the decrease in NM size (e.g. hematite (He et al., 2008), TiO₂ (Zhou et al., 2013)), an increase with the decrease in NM size (e.g. CdSe (Mulvihill et al., 2010), Au NMs (Frens, 1972), Ag NMs (Afshinnia et al., 2017) or independence of CCC of NM size (e.g. Au NMs (Liu et al., 2012)). Similarly, earlier studies on colloid stability reported contradictory results including a decrease (Matthews and Rhodes, 1968; Watillon and Joseph-Petit, 1966; Iler, 1975), an increase (He et al., 2008), an increase followed by a decrease (Ottewill and Shaw, 1966; Kotera et al., 1970), as well as an independence of colloid stability (Elimelech and O'Melia, 1990) on particle size. The discrepancies reported in the literature on size-dependence of CCC are closely related to the size-dependence of zeta potential (Afshinnia et al., 2017). An increase in CCC with decrease in NM size is generally observed when NMs of different sizes possess a constant surface charge, whereas an increase in the CCC with the increase in particle size is observed when the zeta potential increases with particle size. Full discussion of the rational of the effect of NM size on CCC is provided elsewhere (Afshinnia et al., 2017).

5.5. NM dispersity

Currently, no studies have investigated the effect of NM dispersity on the CCC. However, given that the CCC of NM at constant surface potential decrease with the increase in NM size (Afshinnia et al., 2017), size dispersity is likely to significantly influence the CCC for NM suspension. That is in a polydispersed NM suspension, at a given counterion concentration, larger NMs are likely to aggregate in DLA regime whereas small NMs may remain stable or aggregate in RLA regime. For instance, Frens (1972) used this phenomenon to fractionate a mixture of citrate-Au NMs (7.5 and 80 nm) according to particle size by coagulating the larger particles by addition of 30 mM NaNO₃ (Frens, 1972). Therefore, small NMs may remain stable for longer times compared to larger NMs with the same surface potential.

5.6. Surface area

Only few studies investigated the correlation between the CCC and NM specific surface area (SSA). For instance, Zhou et al. reported that the CCC of rutile rods correlated positively with the SSA; that is samples with higher SSA exhibited higher stability (Zhou et al., 2013). In contrast, the CCC of anatase spheres correlated linearly with NM size; that is the CCC increased with the increase in NM size. Nonetheless, the authors also reported a decrease in the CCC with the decrease in rutile rod length, where the CCC tends to a stable value around a length of 50 nm, which is a similar size where the CCC of cit-Ag NMs approaches a constant value (Afshinnia et al., 2017). Interestingly, the electrophoretic mobility of the different rutile rods varied in a narrower range compared to the zeta potential of the anatase spheres, which might explain the differences in the behavior of the two types of TiO₂ NMs. The electrophoretic mobility, and thus zeta potential, of anatase sphere decreases by approximately two folds from the largest to the smallest anatase spheres, which contributes significantly to the reduction in the stability of the small anatase spheres.

Mulvihill reported that the CCC of four different CdSe NMs were found to be linearly correlated to their SSA (Fig. 4a) (Mulvihill et al., 2010). Reevaluating the data reported in this study for spherical CdSe NMs suggests that the CCC decrease with the increase in NM size (Fig. 4b). Similarly, the CCC of all CdSe correlates linearly with the particle size calculated from the specific surface area (Fig. 4c) (Baalousha et al., 2012). It is worth noting that the zeta potential of the spherical CdSe used in this study varies within a narrow range ($ca. -33 \pm 3$ to -35 ± 3 mV). These results are in good agreement with the data observed for cit-Ag NMs (Fig. 4a, and c).

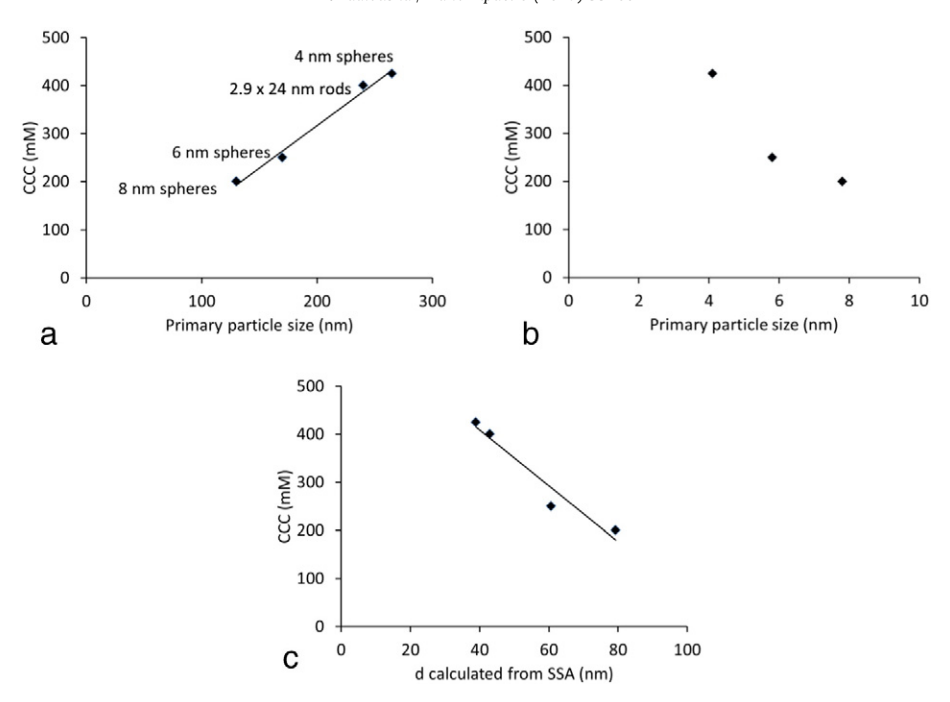


Fig. 4. CCC of CdSe NMs as a function of (a) specific surface area, and (b) primary NM size, and (c) NM diameter calculated from specific surface area. Re-drawn from Mulvihill et al. (2010).

5.7. Heterogeneity of chemical composition and surface structure

NM might purposefully contain (*e.g.* dopants) or acquire (*e.g.* during synthesis process or as a result of sorption processes in natural waters) some impurities, which might play an important role in controlling the electrokinetic properties and colloidal stability of NMs. For instance, The CCC for TiO_2 NMs depends on the concentration of chemical impurities (*e.g.* silicon and phosphorous) introduced during the synthesis process (Liu et al., 2011). This was attributed to the decrease in the pH_{PZC} of TiO_2 with the increase in the concentration of impurities (Si + P) (Liu et al., 2011).

Furthermore, at the atomic level, NM surfaces are heterogeneous in term of chemical composition and structure (e.g. surface roughness and ligand composition and organization) (Baalousha et al., 2010), making it a challenge to quantitatively evaluate and predict surface properties and interfacial processes (Huang et al., 2013). For instance, NMs nearly always have a certain degree of surface roughness on the scale of the Debye length, which under aggregation conditions is on the order of 1 nm in the surrounding electrolyte (Shulepov and Frens, 1996). For instance, reasonable agreement between theoretical attachment efficiencies calculated by DLVO theory and experimentally measured attachment efficiencies could only be obtained if an effective interaction radius, corresponding to surface asperities on TiO₂ particles, was used in the calculations (Snoswell et al., 2005). High resolution TEM images suggested that the effective interaction radius corresponds to the size of surface crystallites formed during synthesis. Additionally, surface roughness influences the dependence of CCC on particle size. For fine roughness, the CCC decreases with increasing particle size (Shulepov and Frens, 1995); whereas, in the case of coarse surface irregularities, the CCC depends on the average configuration of the surface irregularities in the surface area where two double layers overlap. For big particles, this can, in some cases make the CCC increase with the particle size (Shulepov and Frens, 1996). Additionally, the repulsion energy due to the electrical double layer is always larger for rough than for smooth surfaces (Kostoglou and Karabelas, 1995). This should not be confused with the increased particle stability as the particle stability is not only influenced by the repulsion energy, but rather by the total interaction energy and, more specifically, by the height of the energy barrier. In calculating this energy barrier, the influence of surface roughness on van der Waals forces must also be taken into account (Kostoglou and Karabelas, 1995).

Heterogeneity in chemical composition and organization of capping ligands on NM surfaces also plays an important role in controlling NM electrokinetic properties and colloidal stability (Huang et al., 2013). For instance, Au NMs with randomly distributed polar and nonpolar groups have less negative zeta potential values and smaller CCC compared to that of homogenously charged groups, which agree with DLVO prediction. However, when the ligand composition on the surface of Au NMs is the same, particles with nanoscale striates have less negative zeta potential, but much larger CCC compared to particles with disordered surface. The inconsistency of particles with nanoscale striates in their EPM and CCC reflects the complex EDL structure developed in the vicinity of a surface (Huang et al., 2013).

5.8. NM concentration

Several studies have demonstrated the increased NM aggregation rate and the increased aggregate size with the increase in NM concentrations e.g. ZnO (Zhou and Keller, 2010), iron oxides (Baalousha, 2009; He et al., 2008), AuNMs (Baalousha et al., 2016b), etc. However, it has been reported that NM concentration does not affect the attachment efficiency for spherical ZnO NMs (10–100 mg L^{-1}) (Zhou and Keller, 2010). Indeed, this observation is true when NM aggregation is controlled by their physical interactions (e.g. wan der Waals and electrostatic repulsion). However, several NMs have high affinity to media constituents such as anions (Nur et al., 2015; Liang, 1988) and small organic compounds (Afshinnia et al., 2016b). In such circumstances, the attachment efficiency and the CCC values are strongly dependent on NM concentration, in particular at low, environmentally relevant NM concentrations (Afshinnia et al., 2016b). This is because at lower NM concentrations, less total surface area is available, and thus chemical sorption of anions, and bio- and geo-molecules on the surface of NMs is more significant. These chemical sorption processes can result in a significant shift in the surface charge and thus NM aggregation. For instance, Afshinnia et al., reported a concentration-dependent attachment efficiency and CCC values of citrate-Ag NMs in the presence of cystine,

which was attributed to the chemical sorption of cystine to the surface of Ag NMs, resulting in a significant shift in Ag NM surface charge (Afshinnia et al., 2016b). Similarly, carbonate and phosphate anions have high affinity to Ag NMs, sorb to the surface of Ag NMs and reduce the CCC values with the decrease in NM concentration (Afshinnia et al., 2017; Afshinnia and Baalousha, 2016).

5.9. Surface coating composition and coverage

The capping agent is the factor that determines NM stabilization mechanism (see Section 1.4). Physicochemical properties of the capping agent have a greater influence on the aggregation behavior of functionalized Ag NMs than either core composition or their size (Tables S1 and S2) (Liu et al., 2012). Some capping agents such as citrate, SDS, and alginate stabilize NM by electrostatic mechanism (Baalousha et al., 2013; Huynh and Chen, 2011; Zhang et al., 2012b; El Badawy et al., 2012; Lodeiro et al., 2016); whereas other capping agents such as PVP, casein, dextrin, tween, branched polyethyleneimine (BPEI), and Gum Arabic stabilize NMs by steric mechanisms (El Badawy et al., 2012; Lodeiro et al., 2016; Lin et al., 2012). For instance, the CCC values of Ag NMs with different capping agents follow the trend citrate ~ alginate ~ SDS < casein < dextrin < PVP < tween < BPEI ~ gum Arabic (Tables S1 and S2).

Additionally, surface coverage by capping agent plays an important role in determining the stability of NMs. For instance, the CCC of monovalent counterions for PVP-Ag NMs increase with the increase in PVP molecules available to coat the surface of Ag NMs. High capping agent concentrations result in complete coverage of NM surface and thus full steric stabilization, whereas lower capping agent concentrations may result in partial surface coverage and thus electrosteric stabilization (e.g. partial steric stabilization of Ag NMs) (Afshinnia et al., 2017). Increased concentration of human serum albumin (HSA) protein resulted in a reduced attachment efficiency of citrate-Ag NM in K₂SO₄ electrolyte. The attachment efficiency decreased with increasing HSA concentration until the attachment efficiency reached zero which coincided with the HSA concentration required to form a monolayer on the surface of Ag NMs, providing full steric stabilization (Gebauer et al., 2012). Similarly, increased concentration of guar gum (a natural, neutrally charged, nonionic, water-soluble polysaccharide; 0 to 4.0 g L^{-1}) enhanced the stability of zero valent iron NMs (1.5 g L^{-1}); that is resulted in decreased aggregate size (ca. from 500 to 200 nm) (Tiraferri et al., 2008).

Some studies reported CCC for PVP-coated Ag NMs approaching those of electrostatically stabilized Ag NMs (Huynh and Chen, 2011; Zhang et al., 2012b; El Badawy et al., 2012), which can be attributed to the partial surface coverage of Ag NMs by PVP molecules (Afshinnia et al., 2017). These observations highlight the importance of characterizing the surface coverage of NMs by the capping agent.

6. Concluding remarks

This review highlights the role of NM and medium physicochemical properties in controlling NM aggregation kinetics (e.g. α and CCC). These factors are interdependent, rendering it complex to disentangle the correlation between an individual property and NM aggregation kinetics. We found that no single material or media property was a determining factor that control NM aggregation; rather a combination of various material and media physicochemical properties needs to be considered to predict NM aggregation behavior. Correlations between CCC and NM or media property are observed only when all other properties remain constant. Some trends are outlined below for electrostatically-stabilized:

 The CCC increase with the decrease in Hamaker constant, if all other NM properties and media properties are kept constant; Hamaker constant is determined by NM composition and generally follow the order Au $> \text{TiO}_2 > \text{CeO}_2 > \text{Ag} \approx \text{Al}_2\text{O}_3 \approx \text{iron}$ oxides $> \text{ZnO} > \text{B} \approx \text{SiO}_2$. Nonetheless, surface functionalization (*ca.* by citrate, PVP, and humic substances) decreases the Hamaker constant, and thus increases, the CCC of NMs, if all other NM and media properties are kept constant. Yet, surface functionalization of NMs could increase, or decrease their surface charge and therefore might increase, or decrease the CCC irrespective of the influence of surface coating on the Hamaker constant.

- Crystal structure affects NM stability by determining NM Hamaker constant and surface charge (zeta potential).
- The CCC of Ag and Au NMs increases with the decrease in NM size at a
 fixed surface (zeta) potential. This trend is likely to apply for other
 types of NMs, but no data is currently available to generalize this conclusion for all types of NMs. For variable NM surface (zeta) potential,
 the CCC might increase with the increase in NM size, or might be independent of NM size, depending on the change in NM surface charge as
 a function of their size.
- For a polydispersed NM suspensions (ca. Ag and Au), larger NMs aggregate in DLA regime at lower electrolyte concentration compared with smaller NMs, if all size fractions have the same surface charge (zeta potential).
- Counterion complexation can result in an antagonistic effect *e.g.* increased CCC values due to reduction in the counterion valence (*e.g.* Al³⁺ to AlSO₄⁴),
- The CCC is independent of NM concentration for pure electrostatic interactions. However, in the presence of chemical constituents of high affinity to NMs (e.g. Ag NMs in the presence of cystine, carbonate and phosphate anions) that chemisorb on the surface of NMs, the CCC is NM concentration-dependent.
- The CCC of Ag NM increases with the decrease in buffer (e.g. phosphate and carbonate) concentration. This trend is likely to apply for other NMs with high affinity to buffers/ligands due to specific sorption of these buffers/ligands on the surface of NMs and thus alteration of surface (zeta) potential.
- The CCC for Ag NM decreases with light irradiation due to degradation of surface coating and reduction of the magnitude of surface charge.
- The CCC (ca. for CeO₂) increase with the decrease in temperature due to decrease in the magnitude of zeta potential.
- Other NM and media physicochemical properties such as surface area, surface roughness, morphology and surface facets, heterogeneity of chemical composition and surface structure, impurities, dissolved oxygen, also affect the CCC, but, based on the available data in the literature, no general trend can be stated at this stage.

Fully coated, sterically stabilized NMs do not aggregate even in high ionic strength solutions. However, the stability (or CCC) of partially coated NMs decreases with the decrease in surface coverage by the capping agent. Also, sterically stabilized NMs can be destabilized by surface coating replacement, rendering such particles subject to aggregation.

Clearly, the stability of NMs is a complex issue that cannot be described by an individual parameter such as ionic strength, or concentration of NOM, that has been the focus of a significant number of studies in the literature. NM stability is rather determined by a combination of NM and medium physicochemical properties. Chemical interactions of NMs with water constituents such as buffer, anions, cysteine, *etc.* play an equally important role in controlling the stability of NMs, especially at environmentally relevant NM concentrations (*ca.* ng to $\mu g \, L^{-1}$ range).

Although a significant progress has been made in the understanding NM stability, there is still a need for systematic experimental studies especially on the effect of NM and medium physicochemical properties, and the interplay between these factors in order to develop more comprehensive predictive models to estimate NM aggregation kinetics (CCC and α) based on water chemistry and NM physicochemical properties and to further validate the trends summarized above.

Abbreviations

nanomaterials NMs

CCC critical coagulation concentration

attachment efficiency α W stability ratio polyvinylpyrrolidone **PVP**

BPEI branched polyethyleneimine electrophoretic mobility **EPM**

MOPS 3-Morpholinopropanesulfonic acid

Triethanolamine **TEA** Dissolved oxygen DO specific surface area SSA human serum albumin **HSA**

gum Arabic GA

RLA reaction limited aggregation DLA diffusion limited aggregation

 pH_{PZC} point of zero charge

Acknowledgement

We acknowledge funding support from the National Science Foundation (NSF, 1437307, 1553909), the SmartState Centre for Environmental Nanoscience and Risk, and the Arnold School of Public Health at the University of South Carolina.

Appendix A. Supplementary data

Supplementary data to this article can be found online at http://dx. doi.org/10.1016/j.impact.2016.10.005.

References

- Adeleye, A.S., Keller, A.A., 2014. Long-term colloidal stability and metal leaching of single wall carbon nanotubes: effect of temperature and extracellular polymeric substances. Water Res. 49, 236-250.
- Afshinnia, K., Baalousha, M., 2016. Effect of phosphate buffer on aggregation kinetics of citrate-coated silver nanoparticles. NanoImpact (Submitted).
- Afshinnia, K., Sikder, M., Cai, B., Baalousha, M., 2016a. Effect of nanomaterial and media physicochemical properties on Ag NM aggregation kinetics. J. Colloid Interface Sci. 487, 192–200.
- Afshinnia, K., Gibson, I., Merrifield, R., Baalousha, M., 2016b. The concentration-dependent aggregation of Ag NPs induced by cystine. Sci. Total Environ, 557-558, 395-403.
- Afshinnia, K., Sikder, M., Cai, B., Baalousha, M., 2017. Effect of nanomaterial and media physicochemical properties on Ag NM aggregation kinetics. J. Colloid Interface Sci. 487, 192–200.
- Amal, R., Raper, J.A., Waite, T.D., 1992. Effect of fulvic acid adsorption on the aggregation kinetics and structure of hematite particles. J. Colloid Interface Sci. 151 (1), 244–257.
- Assemi, S., Nalaskowski, J., Miller, J.D., Johnson, W.P., 2006. Isoelectric point of fluorite by direct force measurements using atomic force microscopy, Langmuir 22 (4),
- Baalousha, M., 2009. Aggregation and disaggregation of iron oxide nanoparticles: influence of particle concentration, pH and natural organic matter. Sci. Total Environ. 407 (6), 2093-2101.
- Baalousha, M., Manciulea, A., Cumberland, S., Kendall, K., Lead, J.R., 2008. Aggregation and surface properties of iron oxide nanoparticles; influence of pH and natural organic matter. Environ. Toxicol. Chem. 27 (9), 1875–1882.
- Baalousha, M., Le Coustumer, P., Jones, I., Lead, J.R., 2010. Characterization of structural and surface speciation of representative commercially available cerium oxide nanoparticles. Environ. Chem. 7 (4), 377–385.
- Baalousha, M., Lead, J.R., Ju-Nam, Y., 2011a. 3.05 natural colloids and manufactured nanoparticles in aquatic and terrestrial systems. In: Wilderer, P. (Ed.), Treatise on Water Science, Elsevier, Oxford,
- Baalousha, M., Lead, J.R., Ju-Nam, Y., 2011b. Natural colloids and manufactured nanoparticles in aquatic and terrestrial systems. In: Peter, W. (Ed.), Treatise on Water Science. Elsevier, Oxford.
- Baalousha, M., Ju-Nam, Y., Cole, P.A., Gaiser, B., Fernandes, T.F., Hriljac, J.A., Jepson, M.A., Stone, V., Tyler, C.R., Lead, J.R., 2012. Characterization of cerium oxide nanoparticles-part 1: size measurements. Environ. Toxicol. Chem. 31 (5), 983-993.
- Baalousha, M., Nur, Y., Römer, I., Tejamaya, M., Lead, J.R., 2013. Effect of monovalent and divalent cations, anions and fulvic acid on aggregation of citrate-coated silver nanoparticles. Sci. Total Environ. 454-455 (0), 119-131.
- Baalousha, M., Cornelis, G., Kuhlbusch, T.A.J., Lynch, I., Nickel, C., Peijnenburg, W., van den Brink, N.W., 2016a. Modeling nanomaterial fate and uptake in the environment: current knowledge and future trends. Environ. Sci. Nano. 3 (2), 323-345.

- Baalousha, M., Sikder, M., Prasad, A., Lead, I., Merrifield, R., Chandler, G.T., 2016b, The concentration-dependent behavior of nanoparticles. Environ. Chem. 13 (1), 1-3.
- Bennett, S.W., Zhou, D., Mielke, R., Keller, A.A., 2012. Photoinduced disaggregation of TiO₂ nanoparticles enables transdermal penetration. PLoS ONE 7 (11), e48719.
- Bhattacharjee, S., Ko, C.H., Elimelech, M., 1998. DLVO interaction between rough surfaces. Langmuir 14 (12), 3365-3375.
- Borghi, F., Vyas, V., Podestà, A., Milani, P., 2013. Nanoscale roughness and morphology affect the isoelectric point of titania surfaces. PLoS ONE 8 (7), e68655.
- Broide, M.L., Cohen, R.I., 1992. Measurements of cluster-size distributions arising in saltinduced aggregation of polystyrene microspheres. J. Colloid Interface Sci. 153 (2), 493-508
- Buchholz, A., Laskov, C., Haderlein, S.B., 2011. Effects of Zwitterionic buffers on sorption of ferrous iron at goethite and its oxidation by CCl4. Environ, Sci. Technol, 45 (8), 3355-3360
- Buettner, K.M., Rinciog, C.I., Mylon, S.E., 2010. Aggregation kinetics of cerium oxide nanoparticles in monovalent and divalent electrolytes. Colloids Surf. A Physicochem. Eng. Asp. 366 (1–3), 74–79.
- Bullard, J.W., Cima, M.J., 2006. Orientation dependence of the isoelectric point of TiO₂ (ru-
- tile) surfaces. Langmuir 22 (24), 10264–10271.
 Burns, J.L., Yan, Y.D., Jameson, G.J., Biggs, S., 1997. A light scattering study of the fractal aggregation behavior of a model colloidal system. Langmuir 13 (24), 6413-6420.
- Cahill, J., Cummins, P.G., Staples, E.J., Thompson, L., 1986. Aggregate size distribution in flocculating dispersions. Colloids Surf. 18 (2), 189–205. Chegel, V., Rachkov, O., Lopatynskyi, A., Ishihara, S., Yanchuk, I., Nemoto, Y., Hill, J.P., Ariga,
- K., 2012. Gold nanoparticles aggregation: drastic effect of cooperative functionalities in a single molecular conjugate. J. Phys. Chem. C 116 (4), 2683-2690.
- Chen, K.L., Mylon, S.E., Elimelech, M., 2006. Aggregation kinetics of alginate-coated hematite nanoparticles in monovalent and divalent electrolytes. Environ. Sci. Technol. 40 (5), 1516-1523.
- Chen, K.L., Mylon, S.E., Elimelech, M., 2007. Enhanced aggregation of alginate-coated iron oxide (hematite) nanoparticles in the presence of calcium, strontium, and barium cations. Langmuir 23 (11), 5920-5928.
- Chen, Y., Huang, Y., Li, K., 2012. Temperature effect on the aggregation kinetics of CeO₂ nanoparticles in monovalent and divalent electrolytes. J. Environ. Anal. Toxicol. 2 (7) (1000158-1-1000158-5).
- Correa-Duarte, M.A., Giersig, M., Liz-Marzán, L.M., 1998. Stabilization of cds semiconductor nanoparticles against photodegradation by a silica coating procedure. Chem. Phys. Lett. 286, 497-501 (5ΓÇô6).
- Cosgrove, T., 2005. Colloid Science: Principles, Methods and Applications. Blackwell, Oxford.
- Dale, A.L., Lowry, G.V., Casman, E.A., 2013. Modeling nanosilver transformations in freshwater sediments. Environ. Sci. Technol. 47 (22), 12920-12928.
- Dale, A.L., Lowry, G.V., Casman, E.A., 2015a. Much ado about α: reframing the debate over appropriate fate descriptors in nanoparticle environmental risk modeling. Environ, Sci.: Nano 2, 27–32
- Dale, A.L., Casman, E.A., Lowry, G.V., Lead, J.R., Viparelli, E., Baalousha, M., 2015b. Modeling nanomaterial environmental fate in aquatic systems. Environ. Sci. Technol. 49 (5), 2587-2593.
- Derjaguin, B.V., Landau, L.D., 1941. Theory of the stability of strongly charged lyophobic sols and of the adhesion of strongly charged particles in solutions of electrolytes. Acta Physicochim. URSS 14, 633-662.
- Doyen, M., Goole, J., Bartik, K., Bruylants, G., 2016. Amino acid induced fractal aggregation of gold nanoparticles: why and how. J. Colloid Interface Sci. 464, 160-166.
- Einarson, M.B., Berg, J.C., 1993. Electrosteric stabilization of colloidal latex dispersions. J. Colloid Interface Sci. 155 (1), 165-172.
- El Badawy, A.M., Scheckel, K.G., Suidan, M., Tolaymat, T., 2012. The impact of stabilization mechanism on the aggregation kinetics of silver nanoparticles. Sci. Total Environ. 429
- Elimelech, M., O'Melia, C.R., 1990. Effect of particle size on collision efficiency in the deposition of Brownian particles with electrostatic energy barriers. Langmuir 6 (6),
- Elimelech, M., Gregory, J., Jia, G., Williams, R.A., 1995a. Surface interaction potentials. In: Elimelech, M., Gregory, J., Jia, G., Williams, R.A. (Eds.), Particle Deposition and Aggregation: Measurement, Modelling and Simulation. Butterworth-Heinmann, Woburn,
- Elimelech, M., Gregory, J., Jia, X., Williams, R.A., 1995b. Particle Deposition and Aggregation: Measurement, Modelling and Simulation. Butterworth-Heinemann, Oxford.
- Fa, K., Jiang, T., Nalaskowski, J., Miller, J.D., 2003. Interaction forces between a calcium dioleate sphere and calcite/fluorite surfaces and their significance in flotation. Langmuir 19 (25), 10523-10530.
- Fa, K., Paruchuri, V.K., Brown, S.C., Moudgil, B.M., Miller, J.D., 2005. The significance of electrokinetic characterization for interpreting interfacial phenomena at planar, macroscopic interfaces. Phys. Chem. Chem. Phys. 7 (4), 678–684.
- Faure, B., Salazar-Alvarez, G., Bergström, L., 2011. Hamaker constants of iron oxide nanoparticles. Langmuir 27 (14), 8659-8664.
- French, R.H., Cannon, R.M., DeNoyer, L.K., Chiang, Y.M., 1995. Full spectral calculation of non-retarded Hamaker constants for ceramic systems from interband transition strengths. Solid State Ionics 75, 13-33.
- Frenkel, H., Levy, G.J., Fey, M.V., 1992. Organic and inorganic anion effects on reference and soil clay critical flocculation concentration. Soil Sci. Soc. Am. J. 56 (6), 1762–1766.
- Frens, G., 1972. Particle size and sol stability in metal colloids. Kolloid Z. Z. Polym. 250 (7), 736-741.
- Fritz, G., Schadler, V., Willenbacher, N., Wagner, N.J., 2002. Electrosteric stabilization of colloidal dispersions. Langmuir 18 (16), 6381-6390.
- Fuchs, v.N., 1934. Über die Stabilität und Aufladung der Aerosole. Z. Phys. 89 (11-12), 736-743.

- Gaboriaud, F., Ehrhardt, J.J., 2003. Effects of different crystal faces on the surface charge of colloidal goethite ([alpha]-FeOOH) particles: an experimental and modeling study. Geochim. Cosmochim. Acta 67 (5), 967–983.
- Gebauer, J.S., Malissek, M., Simon, S., Knauer, S.K., Maskos, M., Stauber, R.H., Peukert, W., Treuel, L., 2012. Impact of the nanoparticle-protein corona on colloidal stability and protein structure. Langmuir 28 (25), 9673–9679.
- Gedan, H., Lichtenfeld, H., Sonntag, H., Krug, H.J., 1984. Rapid coagulation of polystyrene particles investigated by single-particle laser light scattering. Colloids Surf. 11 (1), 199–207.
- Gilbert, B., Ono, R.K., Ching, K.A., Kim, C.S., 2009. The effects of nanoparticle aggregation processes on aggregate structure and metal uptake. J. Colloid Interface Sci. 339 (2), 285–295
- Giles, D., Lips, A., 1978. Light scattering method for the study of close range structure in coagulating dispersions of equal sized spherical particles. J. Chem. Soc., Faraday Trans. 1 74, 733–744.
- Gorham, J.M., MacCuspie, R.I., Klein, K.L., Fairbrother, D.H., Holbrook, D., 2012. UV-induced photochemical transformations of citrate-capped silver nanoparticle suspensions. J. Nanopart. Res. 14 (10).
- Gregory, J., 2009. Monitoring particle aggregation processes. Adv. Colloid Interf. Sci. 147–148, 109–123.
- Hall, S.B., Duffield, J.R., Williams, D.R., 1991. A reassessment of the applicability of the DLVO theory as an explanation for the Schulze-hardy rule for colloid aggregation. J. Colloid Interface Sci. 143 (2), 411–415.
- He, Y.T., Wan, J., Tokunaga, T., 2008. Kinetic stability of hematite nanoparticles: the effect of particle sizes. J. Nanopart. Res. 10, 321–332.
- Hesterberg, D., Page, A.L., 1990. Flocculation series test yielding time-invariant critical coagulation concentrations of sodium Illite. Soil Sci. Soc. Am. J. 54 (3), 729–735
- Hiemenz, P.C., Rajagopalan, R., 1997. Principles of Colloid and Surface Chemistry. CRC Press. New York. USA.
- Hiemstra, T., van Riemsdijk, W.H., 1999. Effect of different crystal faces on experimental interaction force and aggregation of hematite. Langmuir 15 (23), 8045–8051.
- Ho, C.M., Yau, S.K.-W., Lok, C.N., So, M.H., Che, C.M., 2010. Oxidative dissolution of silver nanoparticles by biologically relevant oxidants: a kinetic and mechanistic study. Chem. Asian. J. 5 (2), 285–293.
- Hotze, E.M., Phenrat, T., Lowry, G.V., 2010. Nanoparticle aggregation: challenges to understanding transport and reactivity in the environment. J. Environ. Qual. 39 (6), 1909–1924.
- Huang, R., Carney, R.P., Stellacci, F., Lau, B.L.T., 2013. Colloidal stability of self-assembled monolayer-coated gold nanoparticles: the effects of surface compositional and structural heterogeneity. Langmuir 29 (37), 11560–11566.
- Huynh, K.A., Chen, K.L., 2011. Aggregation kinetics of citrate and polyvinylpyrrolidone coated silver nanoparticles in monovalent and divalent electrolyte solutions. Environ. Sci. Technol. 45 (13), 5564–5571.
- Iler, R.K., 1975. Coagulation of colloidal silica by calcium ions, mechanism, and effect of particle size. J. Colloid Interface Sci. 53 (3), 476–488.
- Karimian, H., Babaluo, A.A., 2007. Halos mechanism in stabilizing of colloidal suspensions: nanoparticle weight fraction and pH effects. J. Eur. Ceram. Soc. 27 (1), 19–25.
- Kershner, R.J., Bullard, J.W., Cima, M.J., 2004. Zeta potential orientation dependence of sapphire substrates. Langmuir 20 (10), 4101–4108.
- Kim, T., Lee, K., Gong, M.S., Joo, S.W., 2005. Control of gold nanoparticle aggregates by manipulation of Interparticle interaction. Langmuir 21 (21), 9524–9528.
- Kim, T., Lee, C.H., Joo, S.W., Lee, K., 2008. Kinetics of gold nanoparticle aggregation: experiments and modeling. J. Colloid Interface Sci. 318 (2), 238–243.
- Klaine, S.J., Alvarez, P.J.J., Batley, G.E., Fernandes, T.F., Handy, R.D., Lyon, D.Y., Mahendra, S., McLaughlin, M.J., Lead, J.L., 2008. Nanomaterials in the environment: behaviour, fate, bioavailability and effects. Environ. Toxicol. Chem. 27 (9), 1825–1851.
- Kosmulski, M., 2002. The significance of the difference in the point of zero charge between rutile and anatase. Adv. Colloid Interf. Sci. 99 (3), 255–264.
- Kostoglou, M., Karabelas, A.J., 1995. Effect of roughness on energy of repulsion between colloidal surfaces. J. Colloid Interface Sci. 171 (1), 187–199.
- Kotera, A., Furusawa, K., Kudo, M.K., 1970. Colloid chemical studies of polystyrene latices polymerized without any surface-active agents. Kolloid Z. Z. Polym. 240 (1–2), 837–842
- Lesniak, A., Salvati, A., Santos-Martinez, M.J., Radomski, M.W., Dawson, K.A., Aberg, C., 2013. Nanoparticle adhesion to the cell membrane and its effect on nanoparticle uptake efficiency. J. Am. Chem. Soc. 135 (4), 1438–1444.
- Li, K., Zhang, W., Huang, Y., Chen, Y., 2011. Aggregation kinetics of CeO₂ nanoparticles in KCl and CaCl₂ solutions: measurements and modeling. J. Nanopart. Res. 13 (12), 6483–6491.
- Li, Y., Zhang, W., Li, K., Yao, Y., Niu, J., Chen, Y., 2012. Oxidative dissolution of polymer-coated CdSe/ZnS quantum dots under uv irradiation: mechanisms and kinetics. Environ. Pollut. 164, 259–266.
- Li, Y., Zhang, W., Niu, J., Chen, Y., 2013. Surface-coating-dependent dissolution, aggregation, and reactive oxygen species (ROS) generation of silver nanoparticles under different irradiation conditions. Environ. Sci. Technol.
- Liang, L., 1988. Effects of Surface Hemistry on Kinetics of Coagulation of Submicron Iron-Oxide Particles (Alpha-Iron-Oxide) in Water.
- Lichtenbelt, J.T., Pathmamanoharan, C., Wiersema, P.H., 1974a. Rapid coagulation of polystyrene latex in a stopped-flow spectrophotometer. J. Colloid Interface Sci. 49 (2), 281–285.
- Lichtenbelt, J.T., Ras, H.J.M.C., Wiersema, P.H., 1974b. Turbidity of coagulating lyophobic sols. J. Colloid Interface Sci. 46 (3), 522–527.
- Lin, S., Cheng, Y., Liu, J., Wiesner, M.R., 2012. Polymeric coatings on silver nanoparticles hinder autoaggregation but enhance attachment to uncoated surfaces. Langmuir 28 (9), 4178–4186.

- Lips, A., Willis, E., 1973. Low angle light scattering technique for the study of coagulation. J. Chem. Soc., Faraday Trans. 1 69, 1226–1236.
- Lips, A., Smart, C., Willis, E., 1971. Light scattering studies on a coagulating polystyrene latex. Trans. Faraday Soc. 67, 2979–2988.
- Liu, J., Hurt, R.H., 2010. Ion release kinetics and particle persistence in aqueous nano-silver colloids. Environ. Sci. Technol. 44 (6), 2169–2175.
- Liu, L., Moreno, L., Neretnieks, I., 2009a. A novel approach to determine the critical coagulation concentration of a colloidal dispersion with plate-like particles. Langmuir 25 (2) 688–697
- Liu, X., Wazne, M., Christodoulatos, C., Jasinkiewicz, K.L., 2009b. Aggregation and deposition behavior of boron nanoparticles in porous media. J. Colloid Interface Sci. 330 (1), 90–96
- Liu, X., Wazne, M., Han, Y., Christodoulatos, C., Jasinkiewicz, K.L., 2010. Effects of natural organic matter on aggregation kinetics of boron nanoparticles in monovalent and divalent electrolytes. J. Colloid Interface Sci. 348 (1), 101–107.
- Liu, X., Chen, G., Su, C., 2011. Effects of material properties on sedimentation and aggregation of titanium dioxide nanoparticles of anatase and rutile in the aqueous phase. J. Colloid Interface Sci. 363 (1), 84–91.
- Liu, J., Legros, S., Ma, G., Veinot, J.G.C., von der Kammer, F., Hofmann, T., 2012. Influence of surface functionalization and particle size on the aggregation kinetics of engineered nanoparticles. Chemosphere 87 (8), 918–924.
- Lodeiro, P., Achterberg, E.P., Pampin, J., Affatati, A., El-Shahawi, M.S., 2016. Silver nanoparticles coated with natural polysaccharides as models to study AgNP aggregation kinetics using UV-visible spectrophotometry upon discharge in complex environments. Sci. Total Environ. 539, 7–16.
- Loosli, F., Le Coustumer, P., Stoll, S., 2015. Effect of electrolyte valency, alginate concentration and ph on engineered TiO₂ nanoparticle stability in aqueous solution. Sci. Total Environ. 535. 28–34.
- Mahnke, J., Stearnes, J., Hayes, A., Fornasiero, D., Ralston, J., 1999. The influence of dissolved gas on the interactions between surfaces of different hydrophobicity in aqueous media part I. Measurement of interaction forces. Phys. Chem. Chem. Phys. 1 (11), 2793–2798.
- Majedi, S.M., Kelly, B.C., Lee, H.K., 2014. Combined effects of water temperature and chemistry on the environmental fate and behavior of nanosized zinc oxide. Sci. Total Environ. 496. 585–593.
- Masliyah, J.H., Bhattacharjee, S., 2006. Electrokinetic and Colloid Transport Phenomena. John Wiley & Sons.
- Matijevic, E., Allen, L.H., 1969. Interactions of colloidal dispersions with electrolytes. Environ. Sci. Technol. 3 (3), 264–268.
- Matijevic, E., Stryker, L.J., 1966. Coagulation and reversal of charge of lyophobic colloids by hydrolyzed metal ions. J. Colloid Interface Sci. 22 (1), 68–77.
- Matthews, B.A., Rhodes, C.T., 1968. The use of the coulter counter for investigating the coagulation kinetics of mixed monodisperse particulate systems. J. Colloid Interface Sci. 28 (1), 71–81.
- Metin, C.O., Lake, L.W., Miranda, C.R., Nguyen, Q.P., 2010. Stability of Aqueous Silica Nanoparticle Dispersions Under Subsurface Conditions. J. Nanotech. 3, 627–630.
- Metreveli, G., Frombold, B., Seitz, F., Grün, A., Philippe, A., Rosenfeldt, R.R., Bundschuh, M., Schulz, R., Manz, W., Schaumann, G.E., 2016a. Impact of chemical composition of ecotoxicological test media on the stability and aggregation status of silver nanoparticles. Environ. Sci. Nano.
- Metreveli, G., Frombold, B., Seitz, F., Grun, A., Philippe, A., Rosenfeldt, R.R., Bundschuh, M., Schulz, R., Manz, W., Schaumann, G.E., 2016b. Impact of chemical composition of ecotoxicological test media on the stability and aggregation status of silver nanoparticles. Environ. Sci. Nano.
- Misra, S.K., Dybowska, A., Berhanu, D., Croteau, M.N., Luoma, S.N., Boccaccini, A.R., Valsami-Jones, E., 2011. Isotopically modified nanoparticles for enhanced detection in bioaccumulation studies. Environ. Sci. Technol. 46 (2), 1216–1222.
- Misra, N., Kumar, V., Borde, L., Varshney, L., 2013. Localized surface plasmon resonanceoptical sensors based on radiolytically synthesized silver nanoparticles for estimation of uric acid. Sensors Actuators B Chem. 178, 371–378.
- Mittelman, A.M., Fortner, J.D., Pennell, K.D., 2015. Effects of ultraviolet light on silver nanoparticle mobility and dissolution. Environ. Sci. Nano. 2 (6), 683–691.
- Moskovits, M., Vlc ková, B., 2005. Adsorbate-induced silver nanoparticle aggregation kinetics. J. Phys. Chem. B 109 (31), 14755–14758.
- Mulvihill, M.J., Habas, S.E., Jen-La Plante, I., Wan, J., Mokari, T., 2010. Influence of size, shape, and surface coating on the stability of aqueous suspensions of CdSe nanoparticles. Chem. Mater. 22 (18), 5251–5257.
- Napper, D.H., 1977. Steric stabilization. J. Colloid Interface Sci. 58 (2), 390-407
- Ninham, B.W., 1999. On progress in forces since the DLVO theory. Adv. Colloid Interf. Sci. 83 (1–3), 1–17.
- Novich, B.E., Ring, T.A., 1985. Photon correlation spectroscopy of a coagulating suspension of illite platelets. J. Chem. Soc., Faraday Trans. 1 81 (6), 1455–1457.
- Nowicki, W., Nowicka, G., 1994. Verification of the Schulze-hardy rule: a colloid chemistry experiment. J. Chem. Educ. 71 (7), 624.
- Nur, Y., Lead, J.R., Baalousha, M., 2015. Evaluation of charge and agglomeration behavior of TiO₂ nanoparticles in ecotoxicological media. Sci. Total Environ. 535, 45–53.
- Oberndorfer, J., Dobiáš, B., 1989. A collection of papers presented at the 10th European Conference on Chemistry of Interfaces. Adsorption mechanism of anionic surfactants on sparingly soluble minerals. Colloids Surf. 41, 69–76.
- Ortega-Vinuesa, J.L., Martin-Rodriguez, A., Hidalgo-Álvarez, R., 1996. Colloidal stability of polymer colloids with different interfacial properties: mechanisms. J. Colloid Interface Sci. 184 (1), 259–267.
- Ottewill, R.H., Shaw, J.N., 1966. Stability of monodisperse polystyrene latex dispersions of various sizes. Discuss. Faraday Soc. 42 (0), 154–163.
- Parker, J.L., Claesson, P.M., Attard, P., 1994. Bubbles, cavities, and the long-ranged attraction between hydrophobic surfaces. J. Phys. Chem. 98 (34), 8468–8480.

- Peijnenburg, W.J., Baalousha, M., Chen, J., Chaudry, Q., von der Kammer, F., Kuhlbusch, T.A., Lead, J., Nickel, C., Quik, J.T., Renker, M., 2015. A review of the properties and processes determining the fate of engineered nanomaterials in the aquatic environment. Crit. Rev. Environ. Sci. Technol. 45 (19), 2084–2134.
- Pelssers, E.G.M., Stuart, M.C., Fleer, G.J., 1990. Single particle optical sizing (SPOS): II. Hydrodynamic forces and application to aggregating dispersions. J. Colloid Interface Sci. 137 (2), 362–372.
- Penners, N.H.G., Koopal, L.K., 1987. The effect of particle size on the stability of haematite $(\alpha$ -Fe2O3) hydrosols, Colloids Surf. 28, 67–83.
- Petosa, A.R., Jaisi, D.P., Quevedo, I.R., Elimelech, M., Tufenkji, N., 2010. Aggregation and deposition of engineered nanomaterials in aquatic environments: role of physicochemical interactions. Environ. Sci. Technol. 44 (17), 6532–6549.
- Piccapietra, F., Sigg, L., Behra, R., 2012. Colloidal stability of carbonate coated silver nanoparticles in synthetic and natural freshwater. Environ. Sci. Technol. 46 (2), 818–825. Pinchuk, A.O., 2012. Size-dependent Hamaker constant for silver nanoparticles. J. Phys.
- Chem. C 116 (37), 2009–20102.
- Pinchuk, P., Jiang, K., 2015. Size-dependent Hamaker constants for silver and gold nanoparticles. Proc. SPIE 9549. Physical Chemistry of Interfaces and Nanomaterials XIV, 95491J. (Aug. 20) http://dx.doi.org/10.1117/12.2187282.
- Pokhrel, L.R., Dubey, B., Scheuerman, P.R., 2013. Impacts of select organic ligands on the colloidal stability, dissolution dynamics, and toxicity of silver nanoparticles. Environ. Sci. Technol. 47 (22), 12877–12885.
- Reerink, H., Overbeek, J.T., 1954. The rate of coagulation as a measure of the stability of silver iodide sols. Discuss. Faraday Soc. 18, 74–84.
- Rodríguez, K., Araujo, M., 2006. Temperature and pressure effects on zeta potential values of reservoir minerals. J. Colloid Interface Sci. 300 (2), 788–794.
- Römer, I., Wang, Z.W., Merrifield, R.C., Palmer, R.E., Lead, J., 2016. High resolution STEM-EELS study of silver nanoparticles exposed to light and humic substances. Environ. Sci. Technol. 50 (5), 2183–2190.
- Roucoux, A., Schulz, J., Patin, H., 2002. Reduced transition metal colloids: ΓÇë a novel family of reusable catalysts? Chem. Rev. 102 (10), 3757–3778.
- Ryan, J.N., Elimelech, M., 1996. Colloid mobilization and transport in groundwater. Colloids Surf. A Physicochem. Eng. Asp. 107, 1–56.
- Saejiew, A., Grunberger, O., Arunin, S., Favre, F., Tessier, D., Boivin, P., 2004. Critical coagulation concentration of Paddy soil clays in sodium-ferrous iron electrolyte. Soil Sci. Soc. Am. J. 68 (3), 789–794.
- Sani-Kast, N., Scheringer, M., Slomberg, D., Labille, J., Praetorius, A., Ollivier, P., Hungerbühler, K., 2015. Addressing the complexity of water chemistry in environmental fate modeling for engineered nanoparticles. Sci. Total Environ. 535, 150–159.
- Schudel, M., Behrens, S.H., Holthoff, H., Kretzschmar, R., Borkovec, M., 1997. Absolute aggregation rate constants of hematite particles in aqueous suspensions: a comparison of two different surface morphologies. J. Colloid Interface Sci. 196 (2), 241–253.
- Shi, J., Xu, B., Sun, X., Ma, C., Yu, C., Zhang, H., 2013. Light induced toxicity reduction of silver nanoparticles to Tetrahymena pyriformis: effect of particle size. Aquat. Toxicol. 132–133. 53–60.
- Shih, Y.h., Zhuang, C.m., Peng, Y.H., Lin, C.h., Tseng, Y.m., 2012. the effect of inorganic ions on the aggregation kinetics of lab-made TiO₂ nanoparticles in water. Sci. Total Environ. 435, 446–452.
- Shulepov, S.Y., Frens, G., 1995. Surface roughness and the particle size effect on the rate of slow, Perikinetic coagulation. J. Colloid Interface Sci. 170 (1), 44–49.
- Shulepov, S.Y., Frens, G., 1996. Surface roughness and particle size effect on the rate of Perikinetic coagulation: experimental. J. Colloid Interface Sci. 182 (2), 388–394.
- Snoswell, D.R.E., Duan, J., Fornasiero, D., Ralston, J., 2005. Colloid stability of synthetic Titania and the influence of surface roughness. J. Colloid Interface Sci. 286 (2), 526–535.
- Stemig, A.M., Do, T.A., Yuwono, V.M., Arnold, W.A., Penn, R.L., 2014. Goethite nanoparticle aggregation: effects of buffers, metal ions, and 4-chloronitrobenzene reduction. Environ. Sci. Nano. 1 (5), 478–487.
- Stryker, L.J., Matijevic, E., 1969. Counterion complexing and sol stability. II. Coagulation effects of aluminum sulfate in acidic solutions. J. Phys. Chem. 73 (5), 1484–1487.
- Stumm, W., O'Melia, C.R., 1968. Stoichiometry of coagulation. J. Am. Water Works Assoc. 60 (5), 514–539.
- Sun, N., Walz, J.Y., 2001. A model for calculating electrostatic interactions between colloidal particles of arbitrary surface topology. J. Colloid Interface Sci. 234 (1), 90–105.
- Sun, J., Guo, L.H., Zhang, H., Zhao, L., 2014. UV irradiation induced transformation of TiO₂ nanoparticles in water: aggregation and photoreactivity. Environ. Sci. Technol. 48 (20), 11962–11968.

- Tadros, T., 2007. General principles of colloid stability and the role of surface forces. Colloid Stability. Viley-VCH Verlag GmbH, Weinheim Part I.
- Tadros, T.F., 2015. Interfacial Phenomena and Colloid Stability: Industrial Applications.
 Walter de Gruyter GmbH & Co KG.
- Tiraferri, A., Chen, K.L., Sethi, R., Elimelech, M., 2008. Reduced aggregation and sedimentation of zero-valent iron nanoparticles in the presence of guar gum. J. Colloid Interface Sci. 324 (1–2), 71–79.
- Trompette, J.L., Meireles, M., 2003. Ion-specific effect on the gelation kinetics of concentrated colloidal silica suspensions. J. Colloid Interface Sci. 263 (2), 522–527.
- Valdivieso, A.L., Bahena, J.R., Song, S., Urbina, R.H., 2006. Temperature effect on the zeta potential and fluoride adsorption at the α-Al₂O3/aqueous solution Interface. J. Colloid Interface Sci. 298 (1), 1–5.
- Verrall, K.E., Warwick, P., Fairhurst, A.J., 1999. Application of the Schulze-hardy rule to haematite and haematite/humate colloid stability. Colloids Surf. A Physicochem. Eng. Asp. 150 (1–3), 261–273.
- Verwey, E.J.W., Overbeek, J.T.G., 1948. Theory of the Stability of Lyophobic Colloids. Elsevier, Amsterdam.
- Vincent, B., 2012. Early (pre-DLVO) studies of particle aggregation. Adv. Colloid Interf. Sci. 170 (1–2), 56–67.
- Virden, J.W., Berg, J.C., 1992. The use of photon correlation spectroscopy for estimating the rate constant for doublet formation in an aggregating colloidal dispersion. J. Colloid Interface Sci. 149 (2), 528–535.
- Vold, M.J., 1954. Van Der Waals' attraction between anisometric particles. J. Colloid Sci. 9 (5), 451–459.
- Waite, T.D., Cleaver, J.K., Beattie, J.K., 2001. Aggregation kinetics and fractal structure of Γ-alumina assemblages. J. Colloid Interface Sci. 241 (2), 333–339.
- Wang, F., Liu, X., Lu, C.H., Willner, I., 2013. Cysteine-mediated aggregation of Au nanoparticles: the development of a H₂O₂ sensor and oxidase-based biosensors. ACS Nano 7 (8), 7278–7286.
- Watillon, A., Joseph-Petit, A.M., 1966. Interactions between spherical particles of monodisperse polystyrene latices. Discuss. Faraday Soc. 42, 143–153.
- Wijenayaka, L.A., Ivanov, M.R., Cheatum, C.M., Haes, A.J., 2015. Improved parametrization for extended Derjaguin, Landau, Verwey, and Overbeek predictions of functionalized gold nanosphere stability. J. Phys. Chem. C 119 (18), 10064–10075.
- Yakubov, G.E., Butt, H.J., Vinogradova, O.I., 2000. Interaction forces between hydrophobic surfaces. Attractive jump as an indication of formation of "stable" submicrocavities. J. Phys. Chem. B 104 (15), 3407–3410.
- Zakaria, H.M., Shah, A., Konieczny, M., Hoffmann, J.A., Nijdam, A.J., Reeves, M.E., 2013. Small molecule- and amino acid-induced aggregation of gold nanoparticles. Langmuir 29 (25), 7661–7673.
- Zeichner, G.R., Schowalter, W.R., 1979. Effects of hydrodynamic and colloidal forces on the coagulation of dispersions. J. Colloid Interface Sci. 71 (2), 237–253.
- Zhang, Y., Chen, Y., Westerhoff, P., Hristovski, K., Crittenden, J.C., 2008. Stability of commercial metal oxide nanoparticles in water. Water Res. 42 (8–9), 2204–2212.
- Zhang, Y., Chen, Y., Westerhoff, P., Crittenden, J., 2009. Impact of natural organic matter and divalent cations on the stability of aqueous nanoparticles. Water Res. 43 (17), 4249–4257.
- Zhang, W., Yao, Y., Li, K., Huang, Y., Chen, Y., 2011a. Influence of dissolved oxygen on aggregation kinetics of citrate-coated silver nanoparticles. Environ. Pollut. 159 (12), 3757–3762
- Zhang, W., Yao, Y., Sullivan, N., Chen, Y., 2011b. Modeling the primary size effects of citrate-coated silver nanoparticles on their ion release kinetics. Environ. Sci. Technol. 45 (10), 4422–4428.
- Zhang, W., Crittenden, J., Li, K., Chen, Y., 2012a. Attachment efficiency of nanoparticle aggregation in aqueous dispersions: modeling and experimental validation. Environ. Sci. Technol. 46 (13), 7054–7062.
- Zhang, H., Smith, J.A., Oyanedel-Craver, V., 2012b. The effect of natural water conditions on the anti-bacterial performance and stability of silver nanoparticles capped with different polymers. Water Res. 46 (3), 691–699.
- Zhou, D., Keller, A.A., 2010. Role of morphology in the aggregation kinetics of ZnO nanoparticles. Water Res. 44 (9), 2948–2956.
- Zhou, D., Bennett, S.W., Keller, A.A., 2012. Increased mobility of metal oxide nanoparticles due to photo and thermal induced disagglomeration. PLoS ONE 7 (5), e37363.
- Zhou, D., Ji, Z., Jiang, X., Dunphy, D.R., Brinker, J., Keller, A.A., 2013. Influence of material properties on TiO₂ nanoparticle agglomeration. PLoS ONE 8 (11), e81239.